



Influence of basement heterogeneity on the architecture of low subsidence rate Paleozoic intracratonic basins (Reggane, Ahnet, Mouydir and Illizi basins, Hoggar Massif)

Paul Perron¹, Michel Guiraud¹, Emmanuelle Vennin¹, Isabelle Moretti², Éric Portier³, Laetitia Le Pourhiet⁴, and Moussa Konaté⁵

¹Université de Bourgogne Franche-Comté, Centre des Sciences de la Terre, UMR CNRS 6282 Biogéosciences, 6 Bd Gabriel, 21000 Dijon, France

²ENGIE SA, 1, place Samuel de Champlain, Faubourg de l'Arche, 92930 Paris La Défense, France

³Neptune Energy International S.A., 9-11 Allée de l'Arche – Tour EGEE – 92400 Courbevoie, France

⁴Sorbonne Université, CNRS-INSU, Institut des Sciences de la Terre Paris, ISTeP UMR 7193, 75005 Paris, France

⁵Département de Géologie, Université Abdou Moumouni de Niamey, BP:10662, Niamey, Niger

Correspondence: Paul Perron (paul.perron@u-bourgogne.fr, paul.perron@hotmail.fr)

Received: 30 May 2018 – Discussion started: 27 June 2018

Revised: 28 September 2018 – Accepted: 4 October 2018 – Published: 7 November 2018

Abstract. The Paleozoic intracratonic North African Platform is characterized by an association of arches (ridges, domes, swells, or paleo-highs) and low subsidence rate syncline basins of different wavelengths (75–620 km). The Reggane, Ahnet, Mouydir and Illizi basins are successively delimited from east to west by the Amguid El Biod, Arak-Foum Belrem, and Azzel Matti arches. Through the analysis of new unpublished geological data (i.e., satellite images, well logs, seismic lines), the deposits associated with these arches and syncline basins exhibit thickness variations and facies changes ranging from continental to marine environments. The arches are characterized by thin amalgamated deposits with condensed and erosional surfaces, whereas the syncline basins exhibit thicker and well-preserved successions. In addition, the vertical facies succession evolves from thin Silurian to Givetian deposits into thick Upper Devonian sediments. Syndimentary structures and major unconformities are related to several tectonic events such as the Cambrian–Ordovician extension, the Ordovician–Silurian glacial rebound, the Silurian–Devonian “Caledonian” extension/compression, the late Devonian extension/compression, and the “Hercynian” compression. Locally, deformation is characterized by near-vertical planar normal faults responsible for horst and graben structuring associated with folding during the Cambrian–Ordovician–

Silurian period. These structures may have been inverted or reactivated during the Devonian (i.e., Caledonian, Mid–Late Devonian) compression and the Carboniferous (i.e., pre-Hercynian to Hercynian). Additionally, basement characterization from geological and geophysics data (aeromagnetic and gravity maps), shows an interesting age-dependent zonation of the terranes which are bounded by mega-shear zones within the arches–basins framework. The “old” terranes are situated under arches while the “young” terranes are located under the basins depocenter. This structural framework results from the accretion of Archean and Proterozoic terranes inherited from former orogeny (e.g., Pan-African orogeny 900–520 Ma). Therefore, the sedimentary infilling pattern and the nature of deformation result from the repeated slow Paleozoic reactivation of Precambrian terranes bounded by subvertical lithospheric fault systems. Alternating periods of tectonic quiescence and low-rate subsidence acceleration associated with extension and local inversion tectonics correspond to a succession of Paleozoic geodynamic events (i.e., far-field orogenic belt, glaciation).

1 Introduction

Paleozoic deposits fill numerous intracratonic basins, which may also be referred to as “cratonic basins”, “interior cratonic basins”, or “intracontinental sags”. Intracratonic basins are widespread around the world (Heine et al., 2008) and exploration for nonconventional petroleum has revived interest in them. They are located in “stable” lithospheric areas and share several common features (Allen and Armitage, 2011). Their geometries are large circular, elliptical, and/or saucer-shaped to oval. Their stratigraphy is filled with continental to shallow-water sediments. Their subsidence rate is low (5 to 50 m Ma⁻¹) and long (sometimes more than 540 Myr). Their structural framework shows the reactivation of structures and emergence of arches also referred to in the literature as “ridges”, “paleo-highs”, “domes”, and “swells”. Multiple hypotheses and models have been proposed to explain how these slowly subsiding, long-lived intracratonic basins formed and evolved (see Allen and Armitage, 2011 and references therein or Hartley and Allen, 1994). However, their tectonic and sedimentary architectures are often poorly constrained.

The main specificities of intracratonic basins are found on the Paleozoic North Saharan Platform. The sedimentary infilling during ca. 250 Myr is relatively thin (i.e., around a few hundred to a few thousand meters), of great lateral extent (i.e., 9 million km²), and is separated by major regional unconformities (Beuf et al., 1968a, 1971; Carr, 2002; Eschard et al., 2005, 2010; Fabre, 1988, 2005; Fekirine and Abdallah, 1998; Guiraud et al., 2005; Kracha, 2011; Legrand, 2003a). Depositional environments were mainly continental to shallow-marine and homogeneous. Very slow and subtle lateral variations occurred over time (Beuf et al., 1971; Carr, 2002; Fabre, 1988; Guiraud et al., 2005; Legrand, 2003a). The Paleozoic North Saharan Platform is arranged (Fig. 1) into an association of long-lived broad synclines (i.e., basins or subbasins) and anticlines (i.e., arches) of different wavelengths (λ : 75–620 km). Burov and Cloetingh (2009) report deformation wavelengths of the order of 200–600 km when the whole lithosphere is involved and of 50–100 km when the crust is decoupled from the lithospheric mantle. This insight suggests that the inherited basement fabric influences intracratonic basin architecture at a large scale. In addition, pre-existing structures, such as shear zones and terrane suture zones, are present throughout the lithosphere, affecting the geometry and evolution of upper-crustal structural framework forming during later tectonic events (Peace et al., 2018; Phillips et al., 2018).

In this study of the Reggane, Ahnet, Mouydir, and Illizi basins, a multidisciplinary workflow involving various tools (e.g., seismic profiles, satellite images) and techniques (e.g., photogeology, seismic interpretation, well correlation, geophysics, geochronology) has enabled us to (1) make a tectono-sedimentary analysis, (2) determine the spatial arrangement of depositional environments calibrated by bio-

stratigraphic zonation, (3) characterize basin geometry, and (4) ascertain the inherited architecture of the basement and its tectonic evolution. We propose a conceptual coupled model explaining the architecture of the intracratonic basins of the North Saharan Platform. This model highlights the role of basement heritage heterogeneities in an accreted mobile belt and their influence on the structure and evolution of intracratonic basins. It is a first step towards a better understanding of the factors and mechanisms that drive intracratonic basins.

2 Geological setting: the Paleozoic North Saharan Platform and the Reggane, Ahnet, Mouydir, and Illizi basins

The Reggane, Ahnet, Mouydir and Illizi basins (Figs. 1 and 2) are located in southwestern Algeria, north of the Hoggar Massif (Ahaggar). They are depressions filled by Paleozoic deposits. The basins are bounded to the south by the Hoggar Massif (Tuareg Shield) and they are separated one another by the Azzel Matti, the Arak-Foum Belrem, and the Amguid El Biod arches.

Figure 3 synthesizes the lithostratigraphy, the large-scale sequence stratigraphic framework delimited by six main regional unconformities (A to F), and the tectonic events proposed in the literature (cf. references under Fig. 3) affecting the Paleozoic North Saharan Platform.

During the Paleozoic, the Reggane, Ahnet, Mouydir and Illizi basins were part of a set of the supercontinent Gondwana (Fig. 1). This supercontinent resulted from the collision of the West African Craton (WAC) and the East Saharan Craton (ESC), which sandwiched the Tuareg Shield (TS) mobile belt during the Pan-African orogeny (Craig et al., 2008; Guiraud et al., 2005; Trompette, 2000). This orogenic cycle followed by the chain's collapse (ca. 1000–525 Ma) was also marked by phases of oceanization and continentalization (ca. 900–600 Ma) giving rise to the heterogeneous terranes in the accreted mobile belt (Trompette, 2000). The Hoggar Massif is composed of several accreted, sutured, and amalgamated terranes of various ages and compositions resulting from multiple phases of geodynamic events (Bertrand and Caby, 1978; Black et al., 1994; Caby, 2003; Liégeois et al., 2003). Twenty-three well preserved terranes were identified in the Hoggar Massif and grouped into Archean, Paleoproterozoic, and Mesoproterozoic–Neoproterozoic juvenile Pan-African terranes (see legend in Fig. 1). In the West African Craton, the Reguibat Shield is composed of Archean terrains in the west and of Paleoproterozoic terranes in the east (Peucat et al., 2003, 2005).

Then, there is evidence of a complex and polyphased history throughout the Paleozoic (Fig. 3), with alternating periods of quiescence and tectonic activity, individualizing and rejuvenating ancient N–S, NE–SW, or NW–SE structures in arch and basin configurations (Badalini et al., 2002; Boote et al., 1998; Boudjema, 1987; Coward and Ries, 2003; Craig

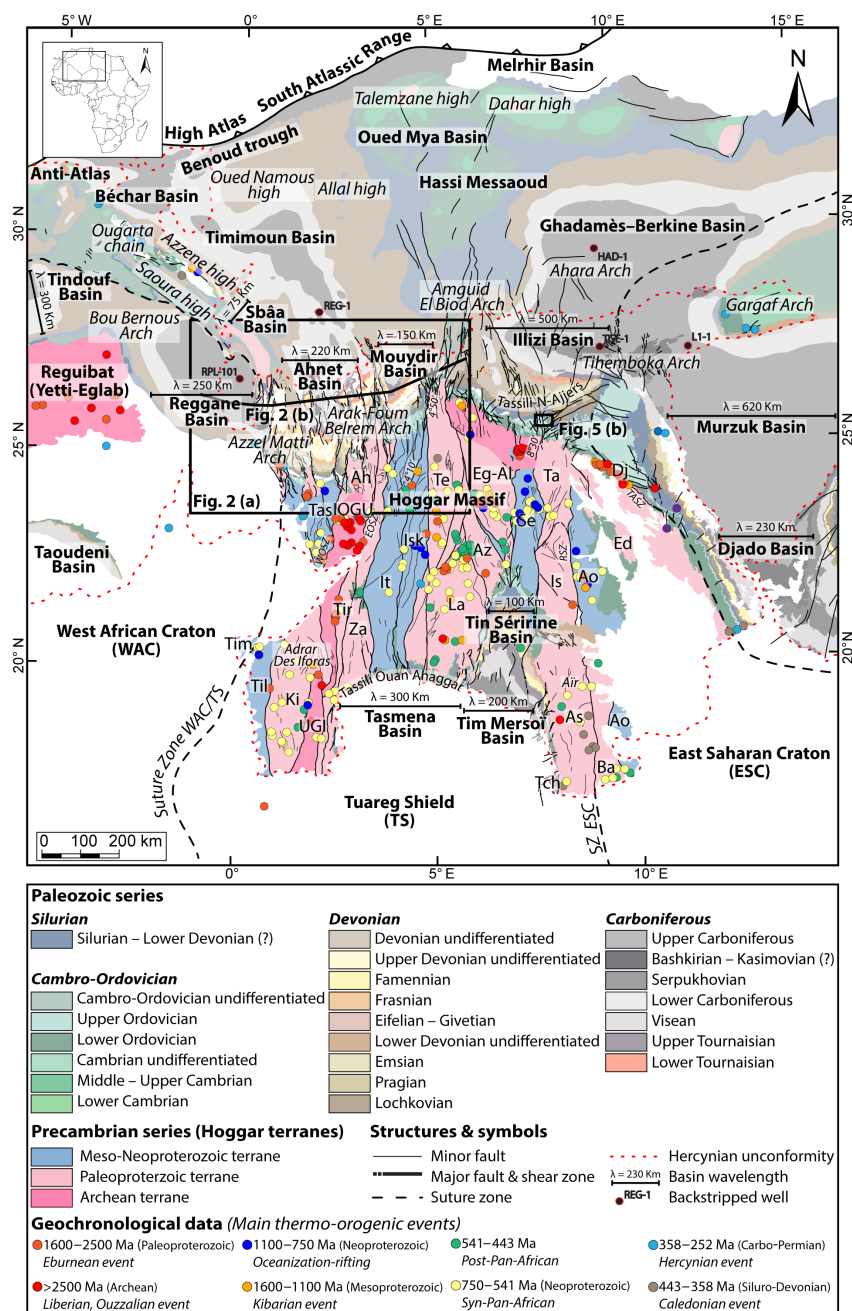


Figure 1. Geological map of the Paleozoic North Saharan Platform (North Gondwana) georeferenced, compiled and modified from (1) a Paleozoic subcrop distribution below the Hercynian unconformity geology of the Saharan Platform (Boote et al., 1998; Galeazzi et al., 2010), (2) a geological map (1/500 000) of the Djado Basin (Jacquemont et al., 1959), (3) a geological map (1/200 000) of Algeria (Bennacef et al., 1974; Bensalah et al., 1971), (4) a geological map (1/50 000) of Air (Joulia, 1963), (5) a geological map (1/2 000 000) of Niger (Greigert and Pognet, 1965), (6) a geological map (1/5 000 000) of the Lower Paleozoic of the central Sahara (Beuf et al., 1971), (7) a geological map (1/1 000 000) of Morocco (Hollard et al., 1985), (8) a geological map of the Djebel Fezzan (Massa, 1988), and (9) a basement characterization of the different terranes from geochronological data compilation (see Supplement) and geological maps (Berger et al., 2014; Bertrand and Caby, 1978; Black et al., 1994; Caby, 2003; Fezaa et al., 2010; Liégeois et al., 1994, 2003, 2005, 2013). Terrane names and abbreviations: Tassendjanet (Tas), Tassendjanet nappe (Tas n.), Ahnet (Ah), In Ouzall Granulitic Unit (IOGU), Iforas Granulitic Unit (UGI), Kidal (Ki), Timétrine (Tim), Tilemsi (Til), Tirek (Tir), In Zaouatene (Za), In Teidini (It), Iskel (Isk), Tefedest (Te), Laouni (La), Azrou-n-Fad (Az), Egéré-Aleskod (Eg-Al), Serouenout (Se), Tazat (Ta), Issalane (Is), Assodé (As), Barghot (Ba), Tchilit (Tch), Aouzegueur (Ao), Edembo (Ed), and Djanet (Dj). Shear zone and lineament names and abbreviations: suture zone East Saharan Craton (SZ ESC), west Ouzall shear zone (WOSZ), east Ouzall shear zone (EOSZ), Raghane shear zone (RSZ), Tin Amali shear zone (TASZ), 4° 10' shear zone, 4° 50' shear zone, and 8° 30' shear zone.

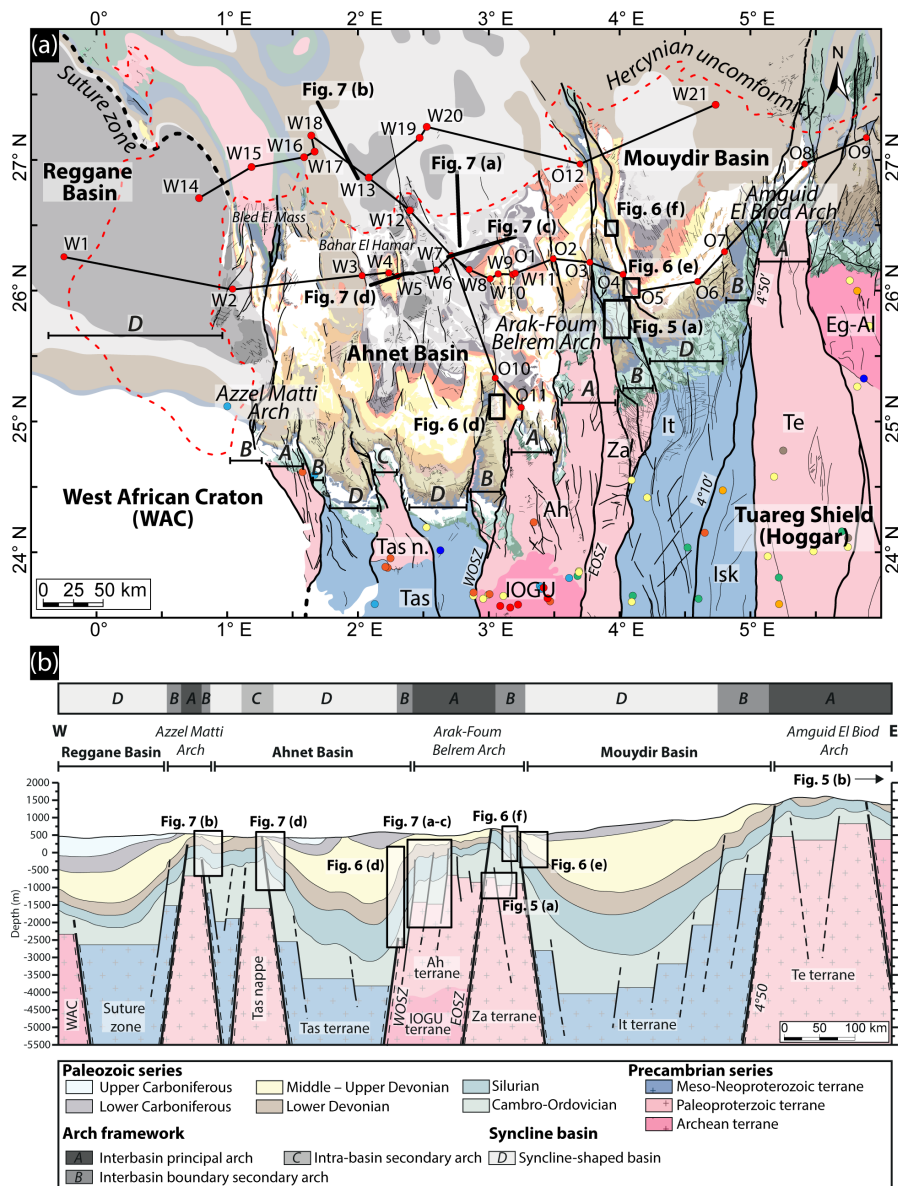


Figure 2. (a) Geological map of the Paleozoic of the Reggane, Ahnet, and Mouydir basins. For the legend and references see Fig. 1. (b) An E–W cross section of the Reggane, Ahnet, and Mouydir basins associated with the different terranes and highlighting the classification of the different structural units. Localization of the interpreted sections (seismic profiles and satellite images). W represents well and O represents outcrop. See Fig. 1 for location of the geological map A and cross section B.

et al., 2008; Guiraud et al., 2005; Logan and Duddy, 1998; Lüning, 2005). The Paleozoic successions of the North Saharan Platform are predominantly composed of siliciclastic detrital sediments (Beuf et al., 1971; Eschard et al., 2005). They form the largest area of detrital sediments ever found on continental crust (Burke et al., 2003), dipping gently NNW (Beuf et al., 1971, 1969; Fabre, 1988, 2005; Fröhlich et al., 2010; Gariel et al., 1968; Le Heron et al., 2009). Carbonate deposits are observed from the Middle–Late Devonian to the Carboniferous (Wendt, 1985, 1988, 1995; Wendt et al., 1993, 1997, 2006, 2009a; Wendt and Kaufmann, 1998). From south

to north, the facies progressively evolve from continental fluvial to shallow marine (i.e., upper to lower shoreface) and then to offshore facies (Beuf et al., 1971; Carr, 2002; Eschard et al., 2005; Fabre, 1988; Fekirine and Abdallah, 1998; Legrand, 1967a).

3 Data and methods

A multidisciplinary approach was used in this study integrating new data (i.e., satellite images, seismic lines and well-

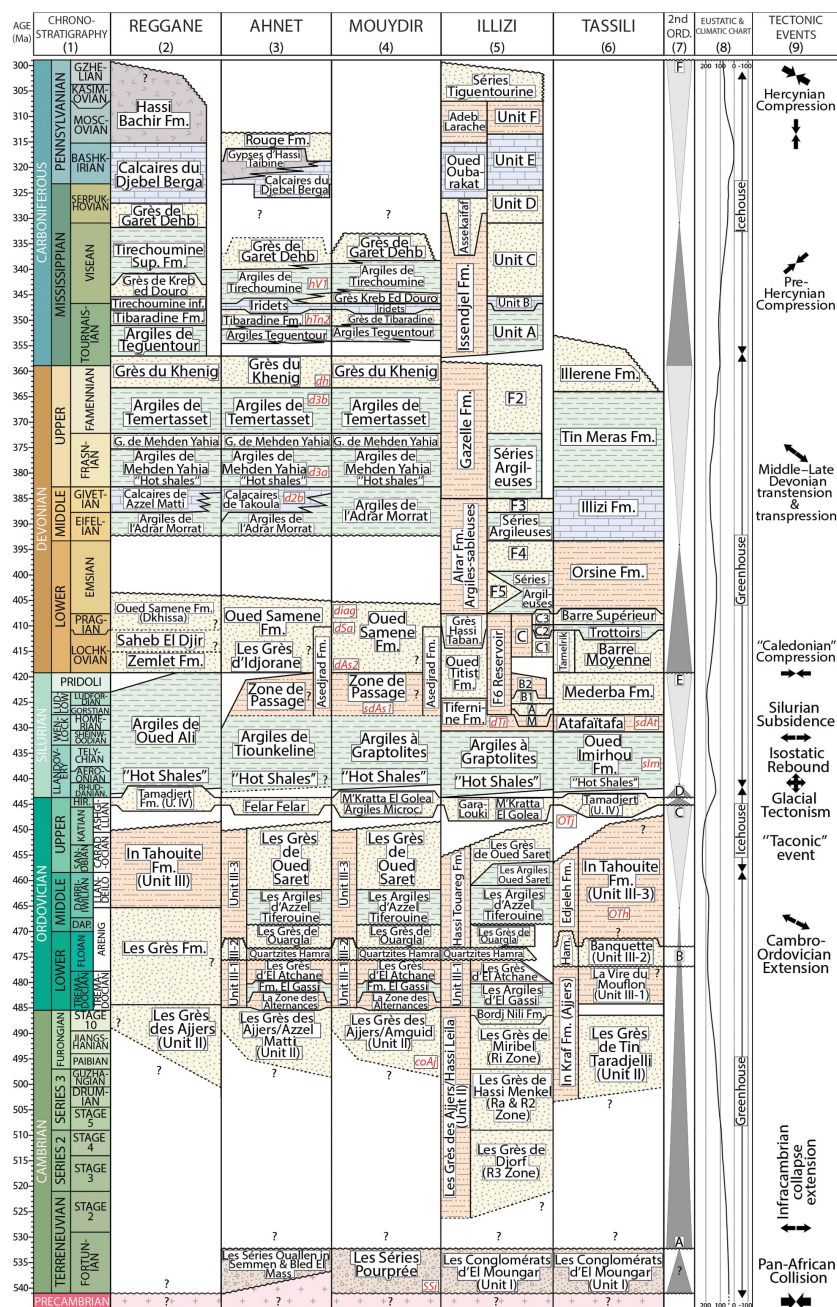


Figure 3. Paleozoic litho-stratigraphic, sequence stratigraphy, and tectonic framework of the north peri-Hoggar basins (North African Saharan Platform) compiled from (1) a chronostratigraphic chart (Ogg et al., 2016), (2) the Cambrian–Silurian (Askri et al., 1995) and the Devonian–Carboniferous stratigraphy of the Reggane Basin (Cózar et al., 2016; Lubeseder, 2005; Lubeseder et al., 2010; Magloire, 1967; Wendt et al., 2006), (3) the Cambrian–Silurian (Paris, 1990; Wendt et al., 2006) and the Devonian–Carboniferous stratigraphy of the Ahnet Basin (Beuf et al., 1971; Conrad, 1973, 1984; Legrand-Blain, 1985; Wendt et al., 2006, 2009a), (4) the Cambrian–Silurian (Askri et al., 1995; Paris, 1990; Videt et al., 2010) and the Devonian–Carboniferous stratigraphy of the Mouydir Basin (Askri et al., 1995; Beuf et al., 1971; Conrad, 1973, 1984; Wendt et al., 2006, 2009a), (5) the Cambrian–Silurian (Eschard et al., 2005; Fekirine and Abdallah, 1998; Jardiné and Yapaoudjian, 1968; Videt et al., 2010) and the Devonian–Carboniferous stratigraphy of the Illizi Basin (Eschard et al., 2005; Fekirine and Abdallah, 1998; Jardiné and Yapaoudjian, 1968), (6) the Cambrian–Silurian (Dubois, 1961; Dubois and Mazelet, 1964; Eschard et al., 2005; Henniche, 2002; Videt et al., 2010) and the Devonian–Carboniferous stratigraphy of the Tassili-N-Ajers (Dubois et al., 1967; Eschard et al., 2005; Henniche, 2002; Wendt et al., 2009a), (7) the sequence stratigraphy of the Saharan Platform (Carr, 2002; Eschard et al., 2005; Fekirine and Abdallah, 1998), (8) a eustatic and climatic chart (Haq and Schutter, 2008; Scotese et al., 1999), and (9) tectonic events (Boudjema, 1987; Coward and Ries, 2003; Craig et al., 2008; Guiraud et al., 2005; Lüning, 2005). (A) Infra-Tassilian (Pan-African) unconformity, (B) intra-Arenig unconformity, (C) Taconic and glacial unconformity, (D) isostatic rebound unconformity, (E) Caledonian unconformity, and (F) Hercynian unconformity.

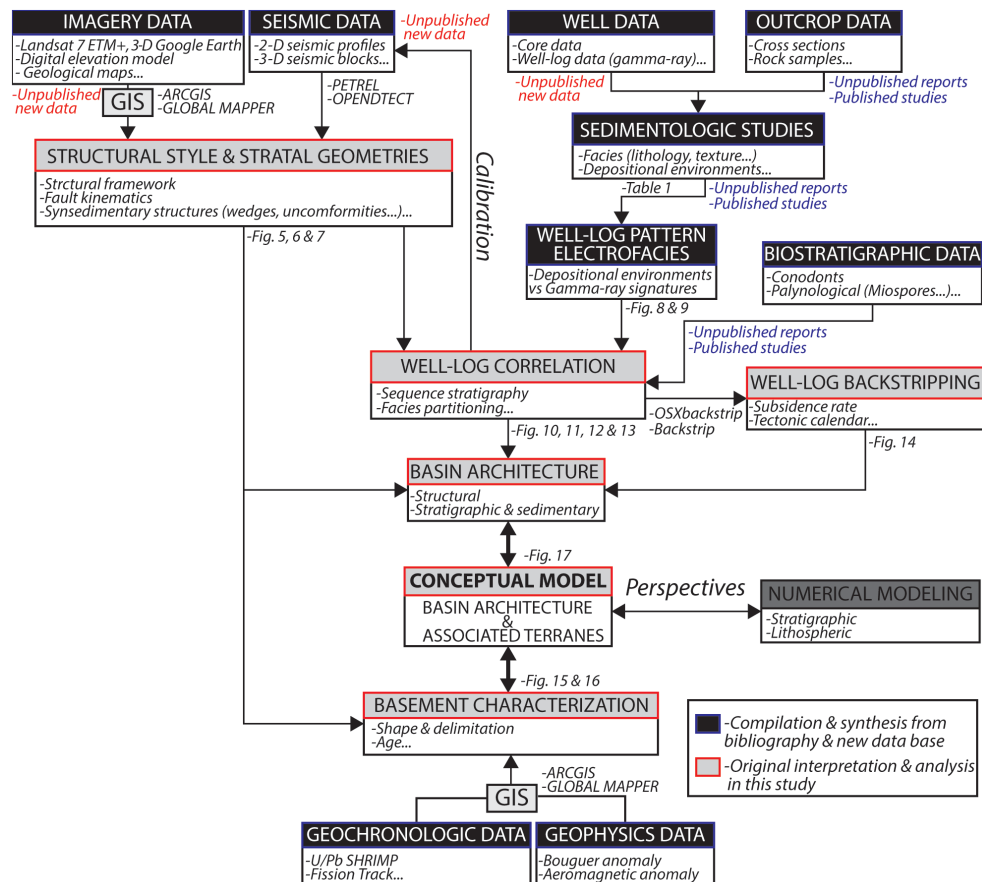


Figure 4. Schematic synthesis of the integrated method of basin analysis in this study.

logs data) in particular from the Reggane, Ahnet, Mouydir, and Illizi basins and the Hoggar Massif (Fig. 4).

The Paleozoic series of the Ahnet and Mouydir basins are well-exposed over an area of approximately 170 000 km² and are well observed in satellite images (Google Earth and Landsat from USGS). Furthermore, a significant geological database (i.e., wells, seismic records, geological reports) has been compiled in the course of petroleum exploration since the 1950s. The sedimentological dataset is based on the integration and analysis of cores, outcrops, well logs, and of lithological and biostratigraphic data. They were synthesized from internal SONATRACH (Dokka, 1999), IFP-SONATRACH consortium reports (Eschard et al., 1999), and published articles (Beuf et al., 1971; Biju-Duval et al., 1968; Wendt et al., 2006). Facies described from cores and outcrops of these studies were grouped into facies associations corresponding to the main depositional environments observed on the Saharan Platform (Table 1). Characteristic gamma-ray (GR) patterns (electrofacies) are proposed to illustrate the different facies associations. The gamma-ray peaks are commonly interpreted as the maximum flooding surfaces (MFS) (e.g., Catuneanu et al., 2009; Galloway, 1989; Milton et al., 1990; Serra and Serra, 2003). Time calibration

of well logs is based on palynomorphs (essentially Chitinozoans and spores) and outcrops on conodonts, graptolites, and brachiopods (Wendt et al., 2006). Palynological data of wells (W1, W7, W12, W19 and W20) from internal unpublished data (Abdesselam-Rouighi, 1991; Azzoune, 1999; Hassan, 1984; Khier, 1974) are based on biozonations from Magloire (1967) and Boumendjel et al. (1988). Well W18 is supported by palynological data and biozonations from Kermadjji et al. (2008).

Synsedimentary extensional and compressional markers are characterized in this structural framework based on the analyses of satellite images (Figs. 5 and 6), seismic profiles (Fig. 7), 21 wells (W1 to W21), and 12 outcrop cross sections (O1 to O12). Wells and outcrop sections are arranged into three E–W sections (Figs. 10, 11 and 12) and one N–S section (Fig. 13). Satellite images (Figs. 5 and 6) and seismic profiles (Fig. 7) are located at key areas (i.e., near arches) illustrating the relevant structures (Fig. 2). The calibration of the key stratigraphic horizon on seismic profiles (Fig. 7) was settled by sonic well-log data using Petrel and OpenTect software. Nine key horizons easily extendable at the regional scale are identified and essentially correspond to major depositional unconformities: near top

Table 1. Synthesis of facies associations (AF1 to AF5), depositional environments, and electrofacies in the Devonian series compiled from internal (Eschard et al., 1999) and published studies (Beuf et al., 1971; Biju-Duval et al., 1968; Wendt et al., 2006).

Facies associations	Criteria & characteristics			Formations	Depositional environments	
	Textures/lithology	Sedimentary structures	Biotic/non-biotic grains			
AF1	Conglomerates, mid to coarse sandstones, siltstones, shales	Trough cross-bedding, mud clasts, lag deposits, fluidal and overturn structures, imbricated grains, lenticular laminations, oblique stratification	Rare oolitic intercalations, imbricated pebbles, sandstones, ironstones, phosphorites, corroded quartz grains, calcareous matrix, brachiopod coquinas, phosphatized pebbles, hematite, azurite, quartz	Oued Samene Fm., Barre Supérieur, Barre Moyenne	Fluvial	Continental (fluvial)
AF2	Silt to argillaceous fine sandstone	Current ripples, climbing ripples, crevasse splay, root traces, paleosols, plant debris	Nodules, ferruginous horizon	Oued Samene Fm., Barre Supérieur, Barre Moyenne	Flood plain	
AF3a	Fine to coarse sandstones, argillaceous siltstones, shales (heterolithic)	Trough cross-bedding, some planar bedding, flaser bedding, mud clasts, mud drapes, root trace, desiccation cracks, water escape, wavy bedding, shale pebble, sigmoidal cross-bedding	Brachiopods, trilobites, tentaculites graptolites	Oued Samene Fm., Grès du Khenig, Barre Supérieur, Barre Moyenne	Delta/estuarine channels	Coastal Plain (transitional marine/continental)
AF3b	Very coarse-grained poorly sorted sandstone	Trough cross-bedding, sigmoidal cross-bedding, abundant mud clasts and mud drapes	Increasing upward bioturbation <i>Skolithos</i> (Sk)	Oued Samene Fm., Grès du Khenig, Barre Supérieur, Barre Moyenne	Fluvial/tidal distributary channels	
AF3c	Fine-grained to very coarse-grained heterolithic sandstone	Sigmoidal cross-bedding with multidirectional tidal bundles, wavy, lenticular, flaser bedding, occasional current and oscillation ripples, occasional mud cracks	Intense bioturbation, <i>Skolithos</i> (Sk), <i>Planolites</i> , (Pl), <i>Thalassinoides</i> (Th)	Talus à Tigillites	Tidal sand flat	
AF3d	Mudstones, varicolored shales, thin sandstone layers	Occasional wave ripples, mud cracks, horizontal lamination, rare multidirectional ripples	Absence of ammonoids, goniatites, calymenids, pelecypod molds, brachiopods coquinas	Oued Samene Fm., Grès du Khenig, Atafaitafa Fm.	Lagoon/mudflat	
AF4a	Silty mudstone associated with coarse to very coarse argillaceous sandstone, poorly sorted, heterolithic silty mudstone	Sigmoidal cross-bedding, abundant mud clasts, wavy, lenticular cross-bedding and flaser bedding, abundant current and oscillation ripples, mud drapes	Shell debris (crinoids, brachiopods)	Oued Samene Fm., Talus à Tigillites	Subtidal	Shoreface
AF4b	Fine- to mid-grained sandstones interbedded with argillaceous siltstone and mudstone, bioclastic carbonates sandstones, brownish sandstones and clays, silts	Oscillation ripples, swaley cross-bedding, bidirectional bedding, flaser bedding, rare hummocky cross-bedding, mud cracks (syneresis), convolute bedding, wavy bedding, combined flow ripples, planar cross low angle stratification, cross-bedding, ripple marks, centimetric bedding, shale pebbles	Ooids, crinoids, bryozoans, coral clasts, fossil debris, stromatopores, tabulates, colonial rugose corals, myriad pelagic stylolites, neritic tentaculitids, brachiopods, iron oolites, abundant micas	Oued Samene Fm., Atafaitafa Fm., Zone de passage, Grès de Mehden Yahia, Calcaires d'Azzel Matti	Open marine–upper shoreface	

Table 1. Continued.

Criteria & characteristics				Formations	Depositional environments	
Facies associations	Textures/lithology	Sedimentary structures	Biotic/non-biotic grains	Ichnofacies		
AF4c	Silty shales to fine sandstones (heterolithic)	Hummocky cross-bedding, planar bedding, combined flow ripples, convolute bedding, dish structures, mud drapes, remnant ripples, flat lenses, slumping	Intense bioturbation, <i>Cruriana</i>	<i>Thalassinoides</i> (Th), <i>Planolites</i> (Pl), <i>Skolithos</i> (Sk), <i>Diplocraterion</i> (Dipl), <i>Teichichnus</i> (Te), <i>Chondrites</i> (Ch), <i>Rogrerella</i> (Ro), <i>Climacichnites</i> (Cl)	Aufaatafia Fm., Zone de passage, Grès de Mehden Yahia, Calcaires d'Azzel Marti	Lower shoreface
AF5a	Grey silty-shales, bundles of skeletal wackestones, silty greenish shale interlayers fine grained sandstones, calcareous mudstones, black shales, polychrome clays (black, brown, grey, green, red, pink), grey and reddish shales	Lenticular sandstones, rare hummocky cross-bedding, mud mounds, mud buildups, low-angle cross-bedding, tempestite bedding, slumping, deep groove marks	Intensive burrowing, bivalve debris, horizontal burrows, skeletal remains (goniatites, orthoconic, nautiloids, stylolinids, trilobites, crinoids, solitary rugose, corals), limestones nodules, ironstone nodules and layers	<i>Zoophycos</i> (Z), <i>Teichichnus</i> (Te), <i>Planolites</i> (Pl)	Argiles à Graptolites, Orsine Fm., Argiles de Mehden Yahia, Argiles de Temertasset	Upper offshore Offshore
AF5b	Black silty-shales (mudstones), bituminous mudstones–wackestones, packstones	Rare structures	Parallel-aligned stylolinids, goniatites, orthoconic nautiloids, pelagic pelecypod <i>Burchiola</i> , anoxic conditions, limestone nodules, goniatites, <i>Burchiola</i> , <i>tenaculitids</i> , ostracods and rare fish remains, <i>Tornoceras</i> , <i>Aulacomoceras</i> , <i>Lobotomoceras</i> , <i>Manticoceras</i> , <i>Costamanticoceras</i> and <i>Virginoceras</i> , graptolites	<i>Zoophycos</i> (Z)	Argiles à Graptolites, Orsine Fm., Argiles de Mehden Yahia, Argiles de Temertasset	Lower offshore

infra-Cambrian, near top Ordovician, near top Silurian, near top Pragian, near top Givetian, near top mid-Frasnian, near top Famennian, near base Quaternary and near Hercynian unconformities (Fig. 7). The stratigraphic layers are identified by the integration of satellite images (Google Earth and Landsat USGS: <https://earthexplorer.usgs.gov/>, last access: 29 November 2016), digital elevation models (DEM), and the 1 : 200 000 geological maps of Algeria (Bennacef et al., 1974; Bensalah et al., 1971).

Subsidence analysis characterizes the vertical displacements of a given sedimentary depositional surface by tracking its subsidence and uplift history (Van Hinte, 1978). The resulting curve details the total subsidence history for a given stratigraphic column (Allen and Allen, 2005; Van Hinte, 1978). Backstripping is also used to restore the initial thicknesses of a sedimentary column (Allen and Allen, 2005; Angevine et al., 1990). Lithologies and paleobathymetries have been defined using facies analysis or literature data. Porosity and the compaction proxy are based on experimental data from (Sclater and Christie, 1980). In this study, subsidence analyses were performed on sections using OSXBackstrip software performing 1D Airy backstripping (following Allen and Allen, 2005; Watts, 2001); available at: <http://www.ux.uis.no/nestor/work/programs.html>, last access: 5 January 2017).

The 800 km² outcrop of basement rocks of the Hoggar Massif provides an exceptional case study of an exhumed mobile belt composed of accreted terranes of different ages. To reconstruct the nature of the basement, a terrane map (Figs. 15 and 16) was put together by integrating geophysical data (aeromagnetic anomaly map: <https://www.geomag.us/>, last access: 1 December 2016, Bouguer gravity anomaly map: <http://bgi.omp.obs-mip.fr/>, last access: 1 December 2016), satellite images (7ETM+ from Landsat USGS: <https://earthexplorer.usgs.gov/>, last access: 29 November 2016) data, geological maps (Berger et al., 2014; Bertrand and Caby, 1978; Black et al., 1994; Caby, 2003; Fezaa et al., 2010; Liégeois et al., 1994, 2003, 2005, 2013), and geochronological data (e.g., U/Pb radiochronology, see Supplement data 1). Geochronological data from published studies were compiled and georeferenced (Fig. 1). Thermo-tectonic ages were grouped into eight main thermotectonic events (Fig. 1): The Liberian-Ouzzalian event (Archean, > 2500 Ma), the Archean, Eburnean (i.e., Paleoproterozoic, 2500–1600 Ma), the Kibarian (i.e., Mesoproterozoic, 1600–1100 Ma), the Neoproterozoic oceanization-rifting (1100–750 Ma), the syn-Pan-African orogeny (i.e., Neoproterozoic, 750–541 Ma), the post-Pan-African (i.e., Neoproterozoic, 541–443 Ma), the Caledonian orogeny (i.e., Siluro-Devonian, 443–358 Ma), and the Hercynian orogeny (i.e., Carbo-Permian, 358–252 Ma).

4 Structural framework and tectono-sedimentary structure analyses

The structural architecture of the North Saharan Platform is characterized by mostly circular to oval shaped basins structured by major faults frequently associated with broad asymmetrical folds displayed by three main trends (Fig. 1): (1) near-N–S, varying from 0 to 10 or 160° N, (2) from 40 to 60° N, and from (3) 100 to 140° N (Figs. 1, 3a, and 4). These fault zones are about 100 km (e.g., faults F1 and F2, Fig. 5) to tens of kilometers long (e.g., faults F3 to F8, Fig. 5). They correspond to the mainly N–S Azzel-Matti, Arak-Foum Belrem, Amguid El Biod, and Tihemboka arches, the NE–SW Bou Bernous, Ahara, and Gargaf arches, and the NW–SE Saoura and Azzene arches (Fig. 1).

4.1 Synsedimentary extensional markers

Extensional markers are characterized by the settlement of steeply westward or eastward-dipping basement normal faults associated with colinear syndepositional folds of several kilometers in length (e.g., Figs. 6a to e and 7a), represented by footwall anticline and hanging wall syncline-shaped forced folds. They are located in the vicinity of different arches (Fig. 2) such as the Tihemboka Arch (Figs. 5b and 6a, b), Arak-Foum Belrem Arch (Figs. 5a, 6c to f and 7a, c), Azzel Matti Arch (Fig. 7b), and Bahar El Hamar area intrabasin arch (Fig. 7d). These tectonic structures can be featured by basement blind faults (e.g., fault F1 in Fig. 7a). The deformation pattern is mainly characterized by brittle faulting in Cambrian–Ordovician series down to the basement and fault-damping in Silurian series (e.g., faults F1 to F6 in Fig. 7b). The other terms of the series (i.e., Silurian to Carboniferous) are usually affected by folding except (see F1 faults in Figs. 6d, 7b, d, and c) where the brittle deformation can be propagated to the Upper Devonian (due to reactivation and/or inversion as suggested in the next paragraph).

In association with the extensional markers, thickness variations and tilted divergent onlaps of the sedimentary series (i.e., wedge-shaped units, progressive unconformities) in the hanging wall syncline of the fault escarpments are observed (Figs. 6 and 7). These are attested using photogeological analysis of satellite images (Fig. 6) and are marked by a gentler dip angle of the stratification planes away from the fault plane (i.e., fault core zone). The markers of syndepositional deformation structures are visible in the hanging-wall synclines of Precambrian to Upper Devonian series (Figs. 6 and 7).

The footwall anticline and hanging-wall syncline-shaped forced folds recognized in this study are very similar to those described in the literature by Grasemann et al. (2005), Khalil and McClay (2002), Schlische (1995), Stearns (1978), Withjack et al. (1990, 2002), and Withjack and Callaway (2000). The wedge-shaped units (DO0 to DO3; Figs. 5, 6, and 7) associated with the hanging-wall synclines are interpreted as

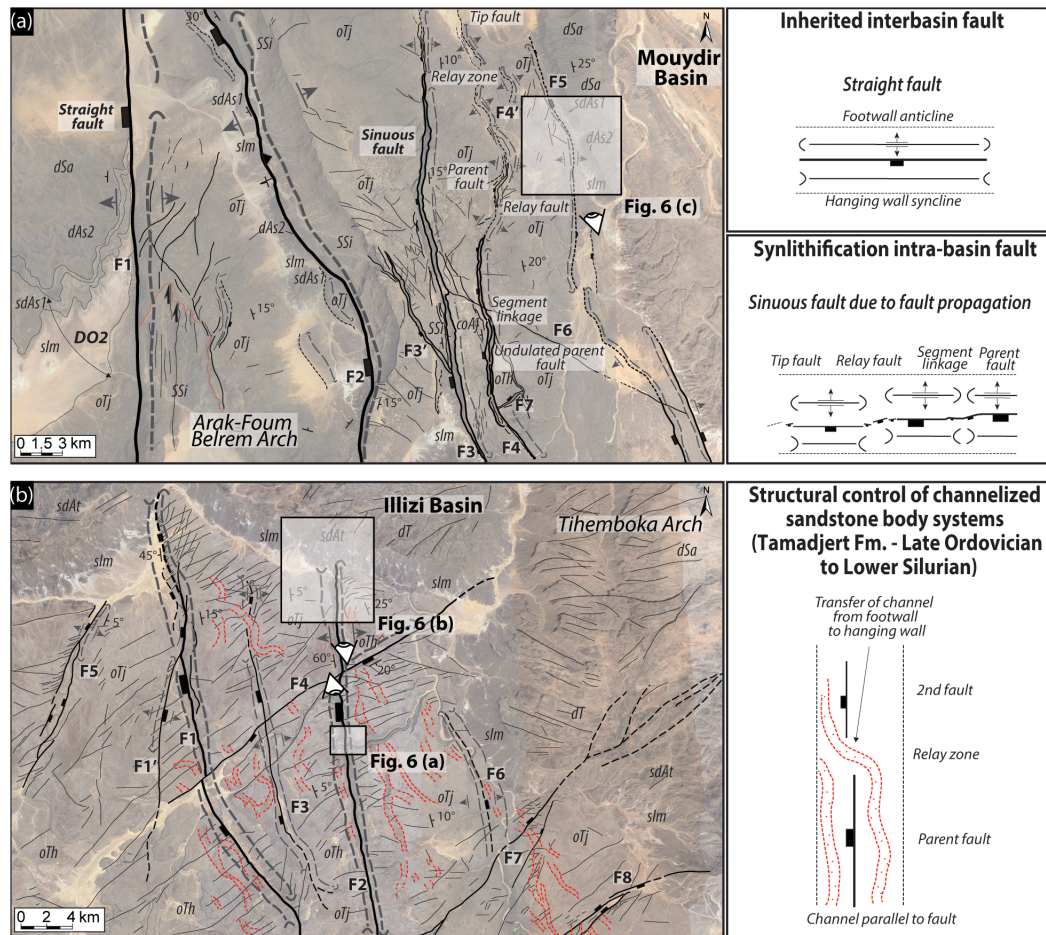


Figure 5. (a) Typology of different types of faults (inherited straight faults vs. sinuous short synlithification propagation faults) in the Cambrian–Ordovician series of the Djebel Settaf (Arak-Foum Belrem Arch; interbasin boundary secondary arch between the Ahnet and Mouydir basins). (b) Structural control of channelized sandstone bodies in Late Ordovician series of South Adrar Assaouatene, Tassili-N-Ajjers (Tihemboka interbasin boundary secondary arch between the Illizi and Murzuq basins). The dotted red line represents Tamadjert Fm. channelized sandstone bodies. The abbreviations used in the figure are as follows: *Oth* – In Tahouite Fm. (Early to Late Ordovician, Floian to Katian); *OTj* – Tamadjert Fm. (Late Ordovician, Hirnantian); *slm* – Imirhou Fm. (Early Silurian); *sdAs1* – Asedjrad Fm. 1 (Late Silurian to Early Devonian); *dAs2* – Asedjrad Fm. 2 (Early Devonian, Lochkovian); *dSa* – Oued Samene Fm. (Lower Devonian, Pragian). See Fig. 2 for map and cross-section location.

synsedimentary normal fault-related folding. The whole tectonic framework forms broad extensional horsts and grabens related to synsedimentary forced folds controlling basin shape and sedimentation.

Following Khalil and McClay (2002), Lewis et al. (2015), Shaw et al. (2005), and Withjack et al. (1990), we use the ages of the growth strata (i.e., wedge-shaped units) to determine the timing of the deformation. The main four wedge-shaped units identified (DO0 to DO3) are indicative of the activation and/or reactivation of the normal faults (extensional settings) during the Neoproterozoic (DO0), the Cambrian–Ordovician (DO1), the Early to Mid-Silurian (DO2), and the Middle to Late Devonian (DO3) times.

In planar view, straight (F1 in Fig. 5a) and sinuous faults (F2, F3, F3', F4, F4', and F5 in Fig. 5a) can be identified.

The sinuous faults are arranged “en echelon” into several segments with relay ramps. These faults are ten to several tens of kilometers long with vertical throws of hundreds of meters that fade rapidly toward the fault tips. The sinuous geometry of normal undulated faults as well as the rapid lateral variation in fault throw are controlled by the propagation and the linkage of growing parent and tip synsedimentary normal faults (Marchal et al., 2003, 1998). We use the stratigraphic age of impacted layers (here Tamadjert Fm.) to date (re)activation of the faults.

According to Holbrook and Schumm (1999), river patterns are extremely sensitive to tectonic structure activity. Here we find that the synsedimentary activity of the extensional structures is also evidenced by the influence of the fault scarp on the distribution and orientation of sinuous channelized sand-

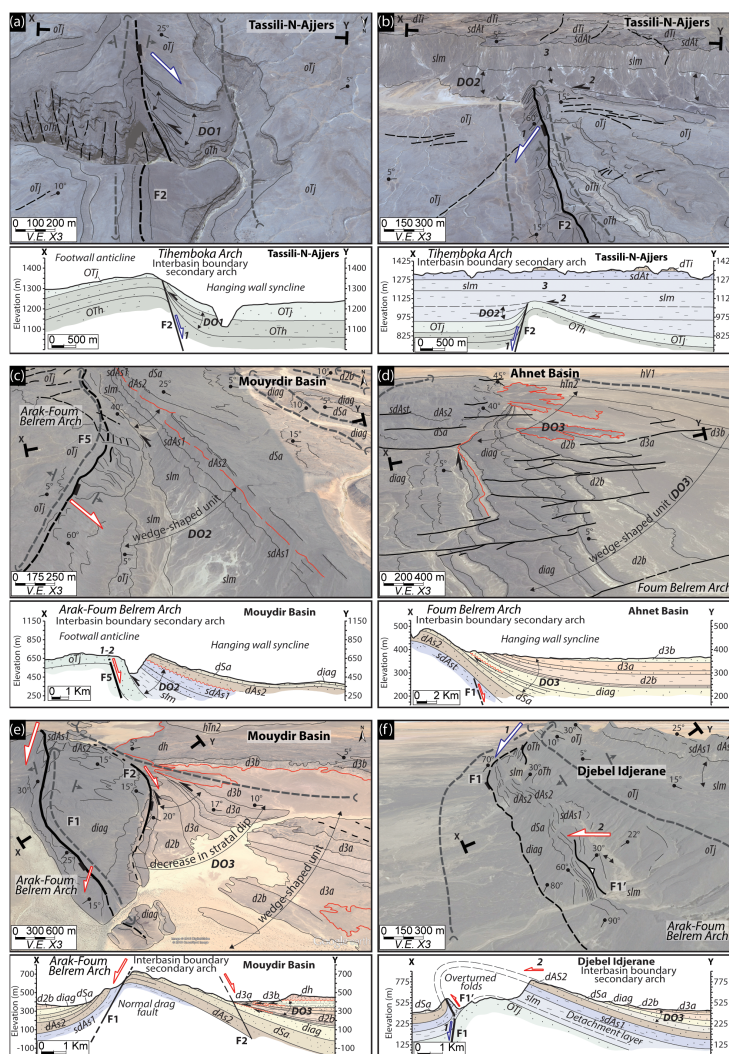


Figure 6. (a) Normal fault (F2) associated with a footwall anticline and a hanging wall syncline with divergent onlaps (i.e., wedge-shaped unit DO1) in the Early to Late Ordovician In Tahouite series (Tassili-N-Ajjers, Tihemboka interbasin boundary secondary arch between the Illizi and Murzuq basins). (b) Ancient normal fault (F2) escarpment reactivated and sealed during Silurian deposition (poly-historic paleo-reliefs) linked to thickness variation, divergent onlaps (DO2) in the hanging wall synclines, and onlaps on the fold hinge anticline (Tassili-N-Ajjers, Tihemboka interbasin boundary secondary arch between the Illizi and Murzuq basins). 1: Early to Late Ordovician extension, 2: Late Ordovician to Early Silurian extension, and 3: Middle to Late Silurian sealing (horizontal drape). (c) Normal fault (F5) associated with forced fold with divergent strata (syncline-shaped hanging wall syncline and associated wedge-shaped unit DO2) and truncation in the Silurian–Devonian series of Djebel Settaf (Arak-Foum Belrem Arch; interbasin boundary secondary arch between the Mouydir and Ahnet basins). 1: Cambrian–Ordovician extension and 2: Silurian–Devonian extensional reactivation (Caledonian extension). (d) Blind basement normal fault (F1) associated with forced fold with in the hanging wall syncline divergent onlaps of the Lower to Upper Devonian series (wedge-shaped unit DO3) and intra-Emsian truncation (Arak-Foum Belrem Arch; interbasin boundary secondary arch between the Mouydir and Ahnet basins). (e) N170° normal blind faults F1 and F2 forming a horst and graben system associated with a forced fold with Lower to Upper Devonian series divergent onlaps (wedge-shaped unit DO3) and intra-Emsian truncation in the hanging-wall syncline (in the Mouydir Basin near Arak-Foum Belrem Arch, eastward interbasin boundary secondary arch). (f) Inherited normal fault (F1) transported from footwall to hanging wall associated with an inverse fault (F1') and accommodated by a detachment layer in the Silurian shales series (thickness variation of Imirhou Fm. between the footwall and hanging wall) and spilled dip strata markers of overturned folding (Djebel Idjerane, Arak-Foum Belrem Arch, eastwards interbasin boundary secondary arch). 1: Cambrian–Ordovician extension and 2: Middle to Late Devonian compression. The abbreviations used in the figure are as follows: *OTh* – In Tahouite Fm. (Early to Late Ordovician, Floian to Katian); *OTj* – Tamadjert Fm. (Late Ordovician, Hirnantian); *slm* – Imirhou Fm. (Early to Mid-Silurian); *sdAt* – Atafaïtafa Fm. (Middle Silurian); *dTi* – Tiferne Fm. (Middle Silurian); *sdAs1* – Asedjrad Fm. 1 (Late Silurian to Early Devonian); *dAs2* – Asedjrad Fm. 2 (Early Devonian, Lochkovian); *dSa* – Oued Samene Fm. (Early Devonian, Pragian); *diag* – Oued Samene shaly-sandstones Fm. (Early Devonian, Emsian?); *d2b* – Givetian; *d3a* – Mehden Yahia Fm. (Late Devonian, Frasnian); *d3b* – Mehden Yahia Fm. (Late Devonian, Famennian); *dh* – Khenig sandstones (late Famennian to early Tournaisian); *hTn2* – late Tournaisian; *hV1* – early Viséan. The red line represents unconformity. See Figs. 1, 2, and 5 for map and cross-section location.

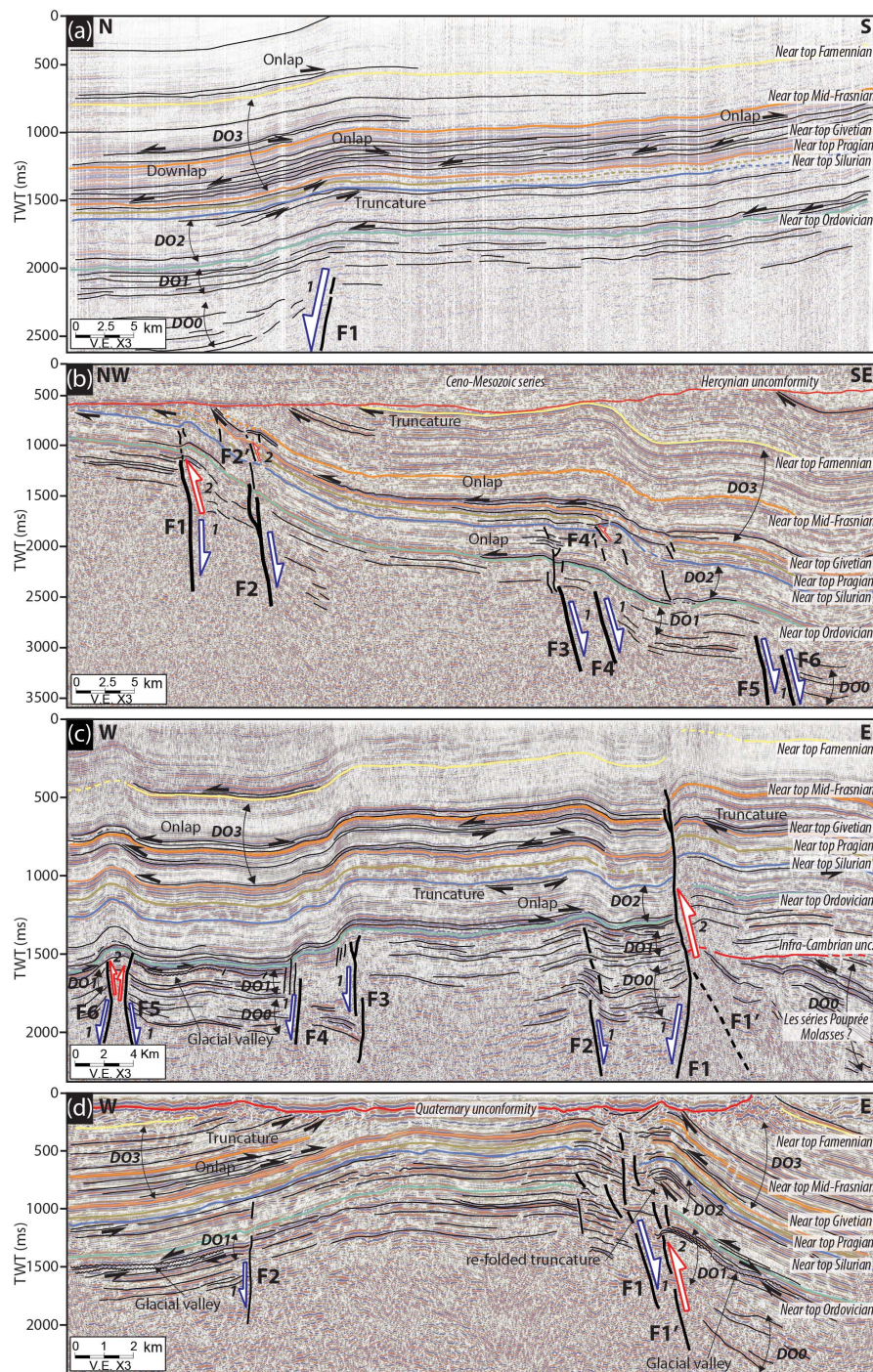


Figure 7. (a) N–S interpreted seismic profile in the Ahnet Basin near Erg Teguntour (near Arak-Foum Belrem Arch, westward interbasin boundary secondary arch) showing steeply dipping northward basement normal blind faults associated with forced folding. (b) NW–SE interpreted seismic profile of near Azzel Matti Arch (interbasin principal arch) showing steeply dipping southeastward basement normal blind faults associated with forced folds. The westernmost structures are featured by reverse fault related propagation fold. (c) W–E interpreted profile of the Ahnet Basin (Arak-Foum Belrem Arch, westward interbasin boundary secondary arch) showing horst and graben structures influencing Paleozoic tectonics associated with forced folds. (d) W–E interpreted seismic profile of Bahar el Hammar in the Ahnet Basin (Ahnet intra-basin secondary arch) showing steeply dipping normal faults F1 and F2 forming a positively inverted horst associated with folding. Multiple activation and inversion of normal faults are correlated with divergent onlaps (wedge-shaped units): D00 infra-Cambrian extension, D01 Cambrian–Ordovician extension, D02 Silurian extension with local Silurian–Devonian positive inversion, and D03 Frasnian–Famennian extension–local compression. See Fig. 2 for map and cross-section location.

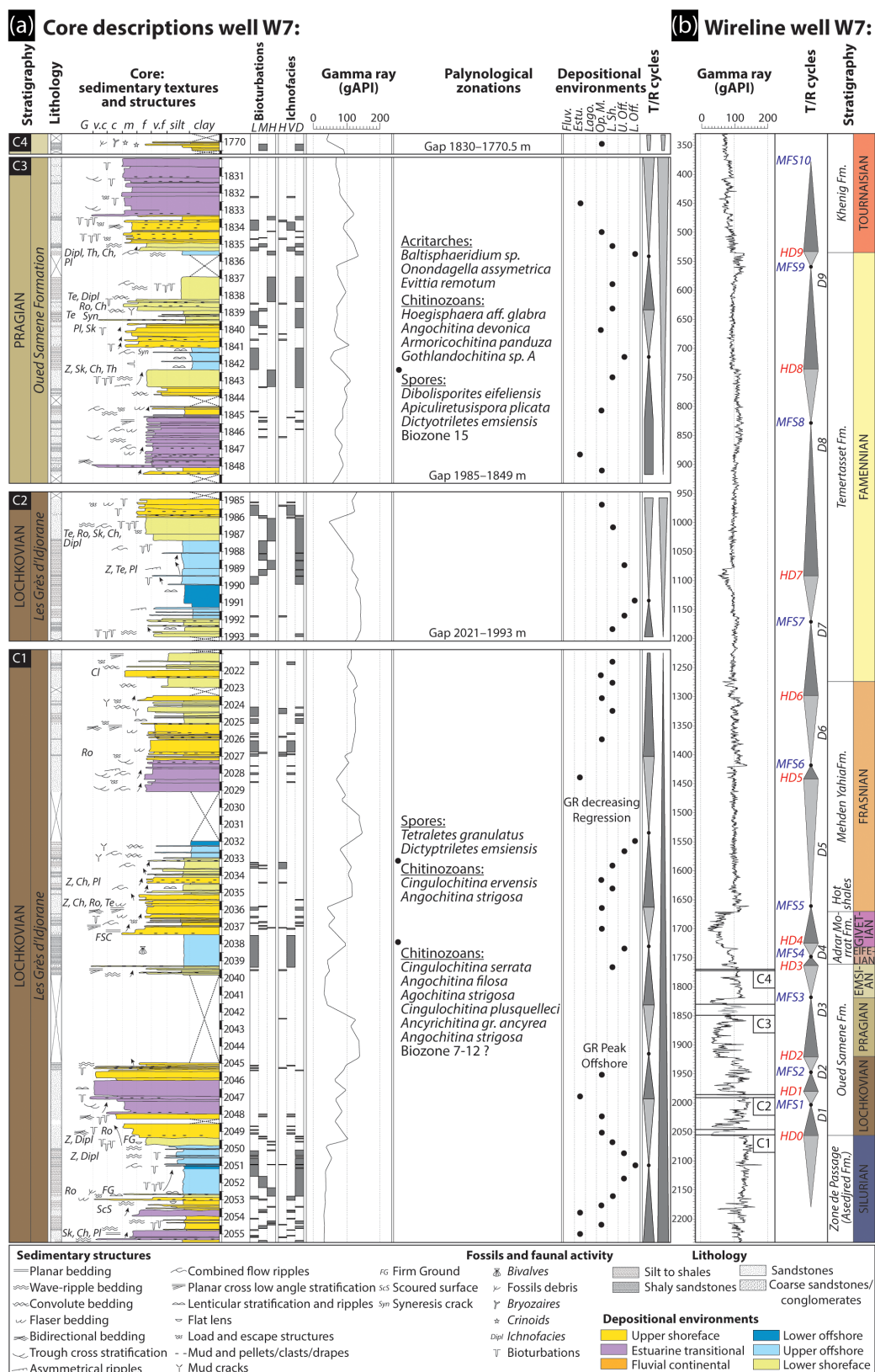


Figure 8. (a) Core description, palynological calibration, and gamma-ray signatures of well W7 modified from an internal core description report (Dokka, 1999) and an internal palynological report (Azzoune, 1999). (b) Devonian sequential stratigraphy of well-log W7. For the location of well W7 see Fig. 2a.

stone body systems (dotted red lines in Fig. 5b). It highlights the (re)activation of the faults during the deposition of these channels, i.e., Late Hirnantian dated by (Girard et al., 2012).

4.2 Synsedimentary compressional markers (inversion tectonics)

After the development of the extensional tectonism described previously, evidence of synsedimentary compressional markers can be identified. These markers are located and preferentially observable near the Arak-Foum Belrem Arch (Fig. 6f; F2 in Fig. 7c), the Azzel Matti Arch (2 in Fig. 7v), and the Bahar El Hamar area intra-basin arch (2 in Fig. 7d). The tectonic structures take the form of inverse faulting reactivating former basement faults (F1' in Fig. 6f, F1 in Fig. 7c, F1' in Fig. 7d, F1 in Fig. 7b). The synsedimentary inverse faulting is demonstrated by the characterization of asymmetric anticlines and is especially observable in satellite images and restricted to the fault footwalls (Fig. 5a along F1–F2).

Landsat image analysis combined with the line drawing of certain seismic lines reveals several thickness variations reflecting divergent onlaps (i.e., wedge-shaped units) which are restricted to the hanging-wall asymmetric anticlines (2 in Figs. 6f, 7b, c and d). The compressional synsedimentary markers clearly post-date extensional divergent onlaps at hanging-wall syncline-shaped forced folds (1 in Figs. 7c, c and d). This architecture is very similar to classical positive inversion structures of former inherited normal faults (Bellahsen and Daniel, 2005; Bonini et al., 2012; Buchanan and McClay, 1991; Ustaszewski et al., 2005). Tectonic transport from the paleo-graben hanging wall toward the paleo-horst footwall (F1, F2–F2', F4–F4' in Fig. 7b; F1–F1' in Fig. 7d) is evidenced. Further positive tectonic inversion architecture is identified by tectonic transport from the paleo-horst footwall to the paleo-graben hanging wall (F1–F1' in Fig. 6f; F1, F5, and F6 in Fig. 7c). This second type of tectonic inversion is very similar to the transported fault models defined by Butler (1989) and Madritsch et al. (2008). The local positive inversions of inherited normal faults occurred during Silurian–Devonian (F4' Fig. 7b) and Middle to Late Devonian times (Figs. 7b, c and d). A late significant compression event between the end of the Carboniferous and the Early Mesozoic was responsible for the exhumation and erosion of the tilted Paleozoic series. This series is related to the Hercynian angular unconformity surface (Fig. 7b).

5 Stratigraphy and sedimentology

The whole sedimentary series described in the literature is composed of fluvial to braid-deltaic plain Cambrian, not only fluvial (e.g., Brahmaputra River analogue), with a transitional facies from continental to shallow marine (Beuf et al., 1968a, b, 1971; Eschard et al., 2005, 2010; Sabaou et al., 2009), Upper Ordovician glaciogenic deposits (Beuf

et al., 1968a, b, 1971; Eschard et al., 2005, 2010), argillaceous deep marine Silurian deposits (Djouder et al., 2018; Eschard et al., 2005, 2010; Legrand, 1986, 2003b; Lüning et al., 2000), and offshore to embayment Carboniferous deposits (Wendt et al., 2009a). In this complete sedimentary succession, we have focused on the Devonian deposits as they are very sensitive to and representative of basin dynamics. The architecture of the Devonian deposits allows us to approximate the main forcing factors controlling the sedimentary infilling of the basin and its synsedimentary deformation. Eleven facies associations organized into four depositional environments (Table 1) are defined to reconstruct the architecture and the lateral and vertical sedimentary evolution of the basins (Figs. 10, 11, 12 and 13).

5.1 Facies association, depositional environments, and erosional unconformities

Based on the compilation and synthesis of internal studies (Eschard et al., 1999), and published papers on the Saharan Platform (Beuf et al., 1971; Eschard et al., 2005, 2010; Heniniche, 2002) and on the Ahnet and Mouydir basins (Biju-Duval et al., 1968; Wendt et al., 2006), eleven main facies associations (AF1 to AF5) and four depositional environments are proposed for the Devonian succession (Table 1). They are associated with their gamma-ray responses (Figs. 8 and 9). They are organized into two continental fluvial (AF1 to AF2), four transitional coastal plain (AF3a to AF3d), three shoreface (AF4a to AF4c), and two offshore (AF5a to AF5b) sedimentary environments.

5.1.1 Continental fluvial environments

This depositional environment features the AF1 (fluvial) and the AF2 (flood plain) facies association (Table 1). Facies association AF1 is mainly characterized by a thinning-up sequence with a basal erosional surface and trough cross-bedded intraformational conglomerates with mud clast lag deposits, quartz pebbles, and imbricated grains (Table 1). It passes into medium to coarse trough cross-bedded sandstones, planar cross-bedded siltstones, and laminated shales. These deposits are associated with rare bioturbation (except at the surface of the sets), ironstones, phosphorites, corroded quartz grains, and phosphatized pebbles. Laterally, facies association AF2 is characterized by horizontally laminated and very poorly sorted silt to argillaceous fine sandstones. They contain frequent root traces, plant debris, well-developed paleosols, bioturbation, nodules, and ferruginous horizons. Current ripples and climbing ripples are associated in prograding thin sandy layers.

In AF1, the basal erosional reworking and high energy processes are characteristic of channel-filling of fluvial systems (Allen, 1983; Owen, 1995). Eschard et al. (1999) identify three fluvial systems (see A, B, and C in Fig. 9) in the Tassili-N-Ajers outcrops: braided dominant (AF1a), meandering

dominant (AF1b), and straight dominant (AF1c). They differentiate them by their different sinuosity, direction of accretion (lateral or frontal), the presence of mud drapes, bioturbation, and giant epsilon cross-bedding. Gamma-ray signatures of these facies associations (A, B, and C in Fig. 9) are cylindrical with an average value of 20 gAPI. The gamma-ray shapes are largely representative of fluvial environments (Rider, 1996; Serra and Serra, 2003; Wagoner et al., 1990). The bottom is sharp with high value peaks and the tops are frequently fining-up, which may be associated with high values caused by argillaceous flood plain deposits and roots (Eschard et al., 1999). AF2 is interpreted as humid flood-plain deposits (Allen, 1983; Owen, 1995) with crevasse splays or preserved levees of fluvial channels (Eschard et al., 1999). Gamma-ray curves of AF2 (D, Fig. 9) show a rapid succession of low to very high peak values, ranging from 50 to 120 gAPI. AF1 and AF2 are typical of the Pragian “Oued Samene” Formation (Wendt et al., 2006). In the Illizi Basin, these facies are mainly recorded in the Ajjers Formation (dated Upper Cambrian? to Ordovician, see Fabre, 2005; Vecoli, 2000; Vecoli et al., 1995, 1999, 2008; Vecoli and Playford, 1997) and the Lochkovian to Pragian “Barre Moyenne” and “Barre Supérieure” formations (Beuf et al., 1971; Eschard et al., 2005).

5.1.2 Transitional coastal plain environments

This depositional environment comprises facies associations AF3a (delta/estuarine), AF3b (fluvial/tidal distributary channels), AF3c (tidal sand flat), and AF3d (lagoon/mudflat) (Table 1). AF3a is mainly dominated by sigmoidal cross-bedded heterolithic rocks with mud drapes. It is also characterized by fine to coarse, poorly sorted sandstones and siltstones often structured by combined flow ripples, flaser bedding, wavy bedding, and some rare planar bedding. Mud clasts, root traces, desiccation cracks, water escape features, and shale pebbles are common. The presence of epsilon bedding is attested, which is formed by lateral accretion of a river point bar (Allen, 1983). The bed surface sets are intensively bioturbated (*Skolithos* and *Planolites*) indicating a shallow marine subtidal setting (Pemberton and Frey, 1982). Faunas such as brachiopods, trilobites, tentaculites, and graptolites are present. AF3b exhibits a fining-up sequence featured by a sharp erosional surface, trough cross-bedded, very coarse-grained, poorly sorted sandstone at the base and sigmoidal cross-bedding at the top (Figs. 8 and 9). AF3c is formed by fine-grained to very coarse-grained sigmoidal cross-bedded heterolithic sandstones with multidirectional tidal bundles. They are also structured by lenticular, flaser bedding and occasional current and oscillation ripples with mud cracks. They reveal intense bioturbation composed of *Skolithos* (Sk), *Thalassinoides* (Th), and *Planolites* (Pl) ichnofacies indicating a shallow marine subtidal setting (Frey et al., 1990; Pemberton and Frey, 1982). AF4d is characterized by horizontally laminated mudstones associated with varicolored shales

and fine-grained sandstones. They exhibit mud cracks, occasional wave ripples, and rare multidirectional current ripples. These sedimentary structures are poorly preserved because of intense bioturbation composed of *Skolithos* (Sk), *Thalassinoides* (Th), and *Planolites* (Pl). The fauna includes ammonoids (rare), goniatites, calymenids, pelecypod molds, and brachiopod coquinas.

In AF3a, both tidal and fluvial systems in the same facies association can be interpreted as an estuarine system (Dalrymple et al., 1992; Dalrymple and Choi, 2007). The gamma-ray signature is characterized by a convex bell shape with rapidly alternating low to mid values (30 to 60 gAPI) due to the mud draping of the sets (see E Fig. 9). These forms of gamma ray are typical of fluvial–tidal influenced environments with upward-fining parasequences (Rider, 1996; Serra and Serra, 2003; Wagoner et al., 1990). AF3a is identified at the top of the Pragian “Oued Samene” Formation and in Famennian “Khenig” Formation (Wendt et al., 2006) in the Ahnet and Mouydir basins. In the Illizi Basin, AF3a is mostly recorded at the top Cambrian of the Ajjers Formation, in the Lochkovian “Barre Moyenne”, and at the top Pragian of the “Barre Supérieure” Formation (Beuf et al., 1971; Eschard et al., 2005). The AF3b association can be characterized by a mixed fluvial and tidal dynamic based on criteria such as erosional basal contacts, fining-upward trends, or heterolithic facies (Dalrymple et al., 1992; Dalrymple and Choi, 2007). They are associated with abundant mud clasts, mud drapes, and bioturbation indicating tidal influences (Dalrymple et al., 1992, 2012; Dalrymple and Choi, 2007). The major difference with the estuarine facies association (AF3a) is the slight lateral extent of the channels which are only visible in outcrops (Eschard et al., 1999). The gamma-ray pattern is very similar to the estuarine electrofacies (see F Fig. 9). AF3c is interpreted as a tidal sand flat laterally present near a delta (Lessa and Masselink, 1995) and associated with an estuarine environment (Leuven et al., 2016). The gamma-ray signature (see G Fig. 9) is distinguishable by its concave funnel shape with alternating low and mid peaks (25 to 60 gAPI) due to the heterogeneity of the deposits and rapid variations in the sand/shale ratio. These facies are observed in the “Talus à Tigillites” Formation of the Illizi Basin (Eschard et al., 2005). In AF4d, both ichnofacies and facies are indicative of tidal mudflat/lagoonal depositional environments (Dalrymple et al., 1992; Dalrymple and Choi, 2007; Frey et al., 1990). The gamma-ray signature has a distinctively high value (80 to 130 gAPI) and an erratic shape (see H Fig. 9). AF4d is observed in the “Atafaitafa” Formation and in the Emsian prograding shoreface sequence of the Illizi Basin (Eschard et al., 2005). It is also recorded in the Lochkovian “Oued Samene” Formation and the Famennian “Khenig” sandstones (Wendt et al., 2006).

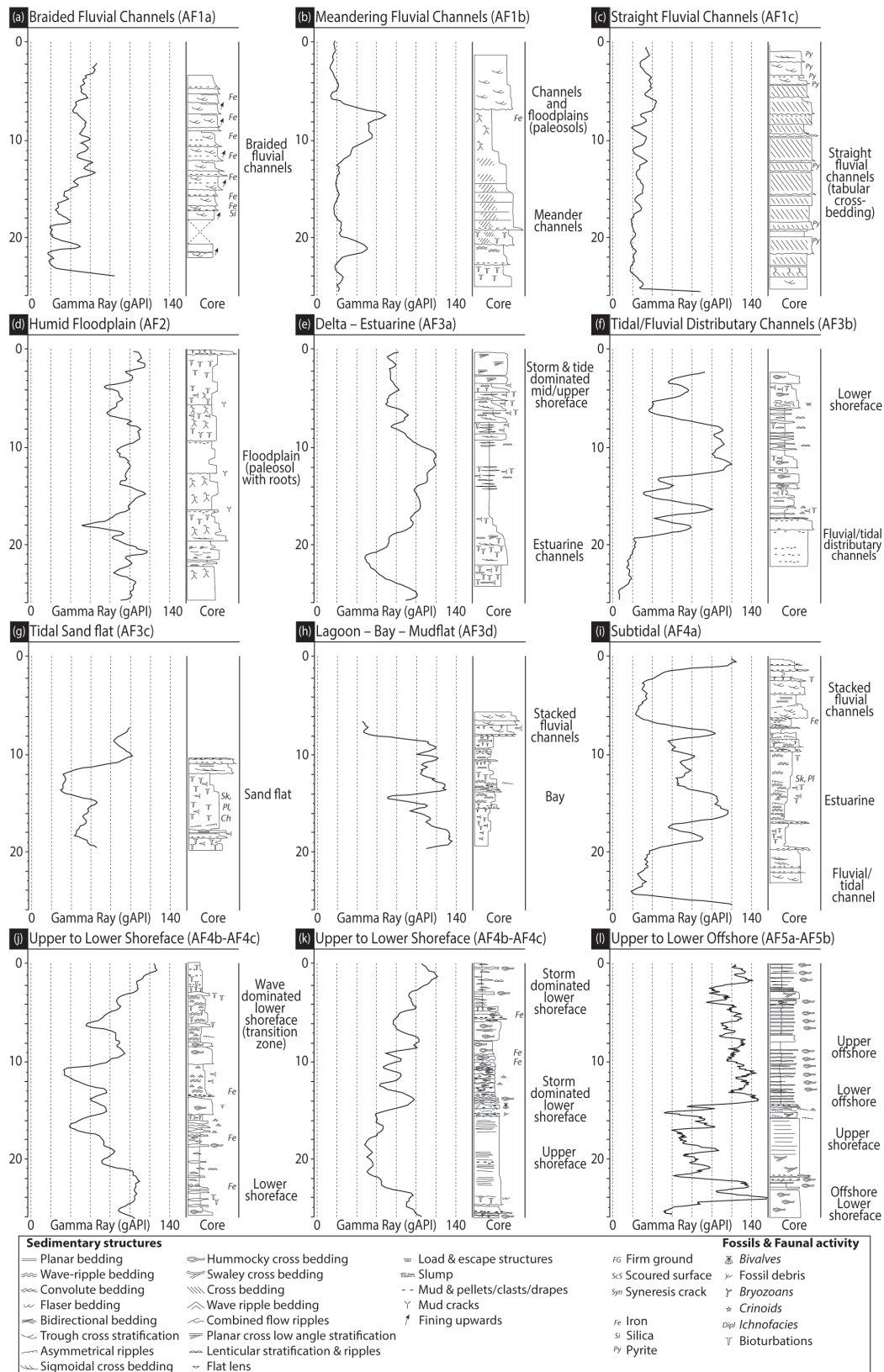


Figure 9. The main depositional environments (a–l) and their associated electrofacies (i.e., gamma-ray patterns) modified and compiled from Eschard et al. (1999).

5.1.3 Shoreface environments

This depositional environment is composed of AF4a (subtidal), AF4b (upper shoreface), and AF4c (lower shoreface) facies associations (Table 1). AF4a is characterized by the presence of brachiopods, crinoids, and diversified bioturbations, by the absence of emersion, and by the greater amplitude of the sets in a dominant mud lithology (Eschard et al., 1999). AF4b is heterolithic and composed of fine to medium-grained sandstones (brownish) interbedded with argillaceous siltstones and bioclastic carbonated sandstones. Sedimentary structures include oscillation ripples, swaley cross-bedding, flaser bedding, cross-bedding, convolute bedding, wavy bedding, and low-angle planar cross-stratification. Sediments were affected by moderate to highly diversified bioturbation by *Skolithos* (Sk), *Cruziana*, *Planolites*, (Pl) *Chondrites* (Ch), *Teichichnus* (Te), *Spirophytons* (Sp) and are composed of ooids, crinoids, bryozoans, stromatoporoids, tabulate and rugose corals, pelagic styliolinids, neritic tentaculitids, and brachiopods. AF4c can be distinguished by a low sand/shale ratio, thick interbeds, abundant hummocky cross-stratification (HCS), deep groove marks, slumping, and intense bioturbation (Table 1).

AF4a is interpreted as a lagoonal shoreface. The gamma-ray pattern (see I Fig. 9) is characterized by a concave bell shape influenced by a low sand/shale ratio with values fluctuating between 100 and 200 gAPI. AF4a is identified in the “Talus à Tigillites” Formation and the Emsian sequence of the Illizi Basin (Eschard et al., 2005) and in the Lochkovian “Oued Samene” Formation (Wendt et al., 2006). AF4b is interpreted as a shoreface environment. The presence of swaley cross-bedding produced by the amalgamation of storm beds (Dumas and Arnott, 2006) and other cross-stratified beds is indicative of upper shoreface environments (Loi et al., 2010). The gamma-ray pattern (see J and K Fig. 9) displays concave erratic egg shapes with a very regularly decreasing-upward trend and ranging from offshore shale with mid values (80 to 60 gAPI) to clean sandstone with lower values at the top (40 to 60 gAPI). AF4b is observed in the “Atafaitafa” Formation corresponding to the “Zone de passage” Formation of the Illizi Basin (Eschard et al., 2005). AF4c is interpreted as a lower shoreface environment (Dumas and Arnott, 2006; Suter, 2006). The gamma-ray pattern displays the same features as the upper shoreface deposits with higher values (i.e., muddier facies) ranging from 100 to 80 gAPI (see J and K Fig. 9).

5.1.4 Offshore marine environments

This depositional environment is composed of AF5a and AF5b facies associations (Table 1). AF5a is mainly defined by wavy to planar-bedded heterolithic silty-shales interlayered with fine-grained sandstones. It also contains bundles of skeletal wackestones and calcareous mudstones. The main sedimentary structures are lenticular sandstones, HCS,

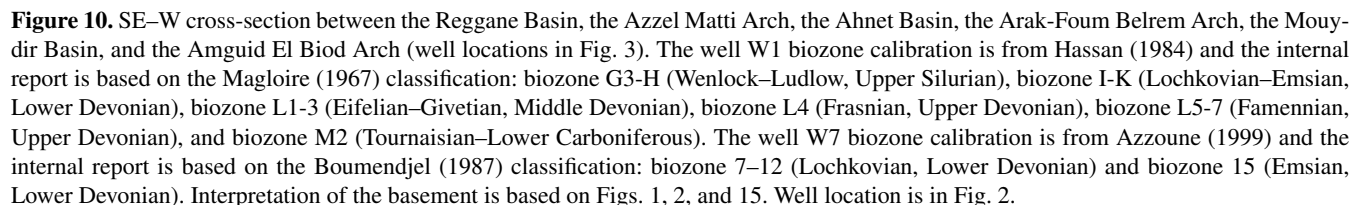
mud mounds, low-angle cross-bedding, tempestite bedding, slumping, and deep groove marks. Sediments can present rare horizontal bioturbation such as *Zoophycos* (Z), *Teichichnus* (Te), and *Planolites* (Pl). AF5b is characterized by an association of black silty shales with occasional bituminous wackestones and packstones. It is composed of graptolites, goniatites, orthoconic nautiloids, pelagic pelecypods, limestone nodules, tentaculitids, ostracods, and rare fish remains. Rare bioturbation such as *Zoophycos* (Z) is visible.

In AF5a, the occurrence of HCS, the decrease in sand thickness and grain size, and the bioturbation and the flora–faunal associations indicate a deeper marine environment under the influence of storms (Aigner, 1985; Dott and Bourgeois, 1982; Reading and Collinson, 2009). AF5a is interpreted as upper offshore deposits (i.e., offshore transitional). The gamma-ray pattern is serrated and erratic with values well grouped around high values from 120 to 140 gAPI (see L Fig. 9). Positive peaks may indicate siltstone to sandstone ripple beds. AF5b is interpreted as lower offshore deposits (Aigner, 1985; Stow et al., 2001; Stow and Piper, 1984). Here again the gamma-ray signature is serrated and erratic with values well grouped around 140 gAPI (see L Fig. 9). Hot shales with anoxic conditions are characterized by gamma-ray peaks (> 140 gAPI). These gamma-ray patterns are typical of offshore environments dominated by shales (Rider, 1996; Serra and Serra, 2003; Wagoner et al., 1990). AF5a and AF5b are observed in the Silurian “Argiles à Graptolites” Formation and the Emsian “Oursine” Formation of the Illizi Basin (Beuf et al., 1971; Eschard et al., 2005; Legrand, 1986, 2003b). The “Argiles de Mehden Yahia” and “Argiles de Temertasset” shales have the same facies (Wendt et al., 2006).

5.2 Sequential framework and unconformities

The high-resolution facies analysis, depositional environments, stacking patterns, and surface geometries observed in the Devonian succession reveal at least two different orders of depositional sequences (large and medium scale, Fig. 8) considered as transgressive/regressive (T/R) (Catuneanu et al., 2009). The sequential framework proposed in Fig. 8b results from the integration of the vertical evolution of the main surfaces (Fig. 8a) and the gamma-ray pattern (Fig. 9). The Devonian series under focus exhibits 9 medium-scale sequences (D1 to D9, Fig. 8; Figs. 10, 11, 12, and 13) bounded by 10 major sequence boundaries (HD0 to HD9), and 9 major flooding surfaces (MFS1 to MFS9). The correlation of the different sequences at the scale of the different basins and arches is used to build three cross sections – two E–W (Figs. 10, 11 and 12) and one N–S (Fig. 13).

The result of the analysis of the general pattern displayed by the successive sequences reveal two major patterns (Figs. 10, 12 and 13) limited by a major flooding surface MFS5. The first pattern extends from the Oued Samene to Adrar Morrat formations and is dated from the Lochko-



vian to Givetian. D1 to D5 medium-scale sequences indicate a general proximal clastic depositional environment (dominated by fluvial to transitional and shoreface facies) with intensive lateral facies evolution. This first pattern is thin (from 500 m in the basin depocenter to 200 m around the basin rim) and with successive amalgamated surfaces on the edge of the arches between the “Zone de passage” and “Oued Samene” formations (e.g., Figs. 10 and 13). It is delimited at the bottom by the HD0 surface corresponding to the Silurian–Devonian boundary. D1 to D3 are composed of T/R sequences with a first deepening transgressive trend indicative of a transition from continental to marine deposits bounded by a major MFS and evolving into a second shallowing trend from deep marine to shallow marine depositional environments. D1 to D3 thin progressively toward the edge and the continental deposits, in the central part of the basin, pass laterally into a major unconformity. The amalgamation of the surfaces and lateral variations of facies between the Ahnet Basin and Azzel Matti and Arak-Foum Belrem arches demonstrate a tectonic control related to the presence of subsiding basins and paleo-highs (i.e., arches).

D4 and D5 display the same T/R pattern with a reduced continental influence and upward decrease in lateral facies variations and thicknesses where the MFS4 marks the beginning of a marine-dominated regime in the entire area. It is identified as the Early Eifelian transgression defined by Wendt et al. (2006). The D5 sequence is mainly composed of shoreface carbonates. Evidence of mud mounds preferentially located along faults are well-documented in the area for that time (Wendt et al., 1993, 1997, 2006; Wendt and Kaufmann, 1998). This change in the general pattern indicates reduced tectonic influence.

MFS5, at the transition between the two main patterns, represents a major flooding surface on the platform and is featured worldwide by deposition of “hot shales” during the early Frasnian (Lüning et al., 2003, 2004; Wendt et al., 2006).

The second pattern extends from the “Mehden Yahia”, “Temertasset” to the “Khenig” formations dated Frasnian to Lower Tournaisian. This pattern is composed of part of D5–D9 medium-scale sequences. It corresponds to homogeneous offshore depositional environments with no lateral facies variations. However, local deltaic (fluvio–marine) conditions are observed during the Frasnian at the Arak Foum Belrem Arch (“Grès de Mehden Yahia” in Fig. 12). A successive alternation of shoreface and offshore deposits is organized into five medium-scale sequences (part of D5, and D6 to D9; Figs. 10, 11 and 12). They, in particular, show some regressive phases with the deposition of both “Grès de Mehden Yahia” and “Grès du Khnig” sandstones (bounded by HD6 and HD9). This pattern (i.e., part of D5 to D9) corresponds to the general maximum flooding (Lüning et al., 2003, 2004; Wendt et al., 2006) under eustatic control with no tectonic influences.

6 Subsidence and tectonic history: an association of low rate extensional subsidence and positive inversion pulses

The backstripping approach (Fig. 14) was applied to five wells (W1, W5, W7, W17, and W21). The morphology of the backstripped curve and subsidence rates can provide clues as to the nature of the sedimentary basin (Xie and Heller, 2009). In intracratonic basins, reconstructed tectonic subsidence curves are almost linear to gently exponential in shape, similar to those of passive margins and rifts (Xie and Heller, 2009). The compilation of tectonic backstripped curves from several wells in peri-Hoggar basins (Fig. 14a, see Fig. 1 for location) and from wells in the study area (Fig. 14b) display low rates of subsidence (from 5 to 50 m Myr^{−1}) organized in subsidence patterns of: inversion of the low rate subsidence (ILRS type c, red line, Fig. 14c), deceleration of the low rate subsidence (DLRS type b, black line), and acceleration of the low rate subsidence (ALRS type a, blue line).

Each period of ILRS, DLRS, and ALRS may be synchronous among the different wells studied (see B1 to J, Fig. 14b) and some wells from published data (see D to J Fig. 14a).

The Saharan Platform is marked by a rejuvenation of basement structures, around arches (Figs. 1, 2, and 3), linked to regional geodynamic pulses during Neoproterozoic to Paleozoic times (Fig. 14). A compilation of the literature shows that the main geodynamic events are associated with discriminant association of subsidence patterns:

- a. Late Pan-African compression and collapse (patterns a, b, and c, A Fig. 14a). The infra-Cambrian (i.e., top Neoproterozoic) is characterized by horst and graben architecture associated with wedge-shaped unit DO0 in the basement (Fig. 7). This structuring, probably related to Pan-African post-orogenic collapse, is illustrated by intracratonic basins infilled with volcano-sedimentary molasses series (Ahmed and Moussine-Pouchkine, 1987; Coward and Ries, 2003; Fabre et al., 1988; Oudra et al., 2005).
- b. Cambrian–Ordovician geodynamic pulse (Fig. 14). Highlighted by the wedge-shaped units DO1 (Figs. 6a and 7), the horst and graben system is correlated with deceleration (DLRS pattern a, B1) and with local acceleration of the subsidence (ALRS pattern b, B2). The Cambrian–Ordovician extension is documented on arches (Arak-Foum Belrem, Azzel Matti, Amguid El Biod, Tihemboka, Gargaf, Murizidié, Dor El Gussa, etc.) of the Saharan Platform by synsedimentary normal faults, reduced sedimentary successions (Bennacef et al., 1971; Beuf et al., 1968a, b, 1971; Beuf and Montadert, 1962; Borocco and Nyssen, 1959; Claracq et al., 1958; Echikh, 1998; Eschard et al., 2010; Fabre, 1988; Ghienne et al., 2003, 2013; Zazoun and Mahdjoub, 2011), and by stratigraphic hiatuses (Mélou et al.,

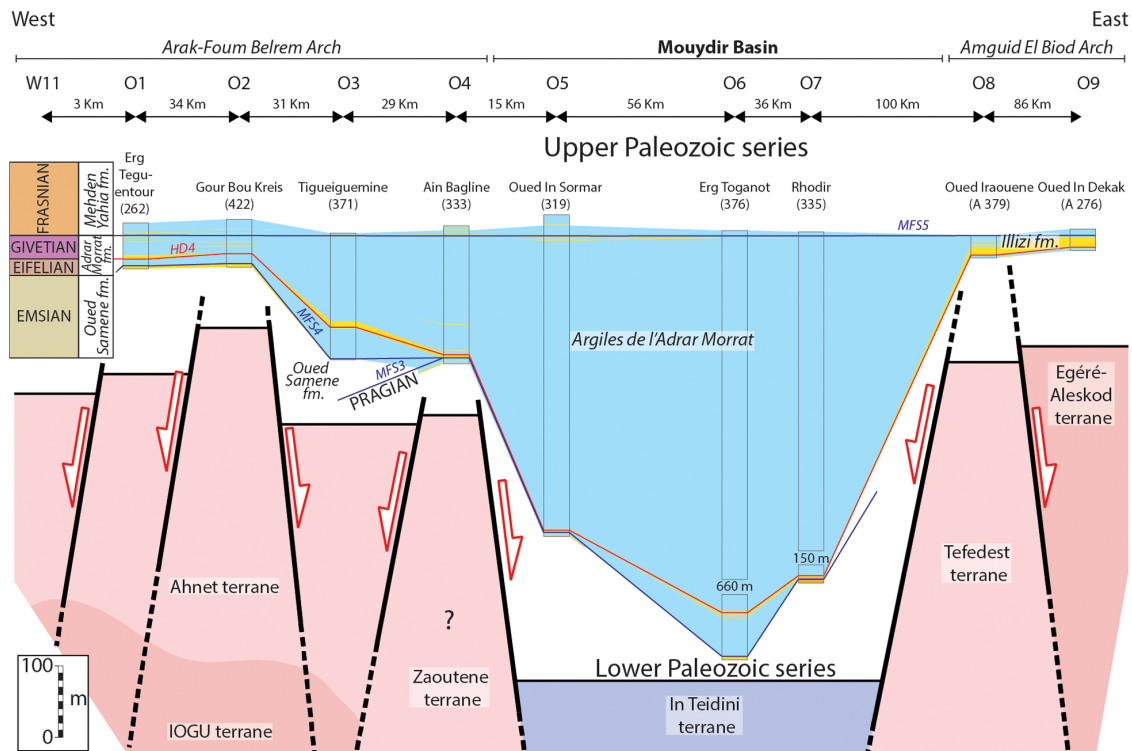


Figure 11. SE–W cross section between the Arak-Foum Belrem Arch, the Mouydir Basin, and the Amguid El Biod Arch. Outcrop cross-section correlations and biostratigraphic calibrations are based on the compilation of published papers (Wendt et al., 2006, 2009b). Interpretation of the basement is based on Figs. 1, 2, and 15. Outcrop location is in Fig. 2.

1999; Oulebsir and Paris, 1995; Paris et al., 2000; Vecoli et al., 1995, 1999).

- c. Late Ordovician geodynamic pulse (i.e., Hirnantian glacial and isostatic rebound; Fig. 14). Late Ordovician incisions mainly situated at the hanging walls of normal faults (Fig. 7c and d) are interpreted as Hirnantian glacial-paleovalleys (Le Heron, 2010; Smart, 2000) and followed by local inversion of low rate subsidence (ILRS of type c, C in Fig. 14).
- d. Silurian extensional geodynamic pulse (D, Fig. 14). The Silurian post-glaciation period is featured by the reactivation and sealing of the inherited horst and graben fault system (i.e., wedge-shaped unit DO2; Figs. 6b, c, 7a and b). It is linked to an acceleration of the subsidence (ALRS of pattern b in Fig. 14). This tectonic extension is documented in seismic records (Najem et al., 2015) and is associated with the Silurian major transgression on the Saharan Platform (e.g., Eschard et al., 2005; Lüning et al., 2000).
- e. Late Silurian to Early Devonian geodynamic pulse (Caledonian compression; E Fig. 14). Late Silurian times are marked by reactivation and local positive inversion of the former structures (Figs. 6c and 7b);

this occurs due to truncations located at fold hinges (Figs. 6c and 7) and due to a major shift from marine to fluvial/transitional environments (e.g., Fig. 10). Back-stripped curves register an inversion of the subsidence (ILRS of pattern c, in Fig. 14). The Caledonian event is mentioned as related to large-scale folding or uplifted arches (e.g., the Gargaff, Tihemboka, Ahara, Murizidé-Dor el Gussa and Amguid El Biod arches) and it is associated with breaks in the series and with angular unconformities (Beuf et al., 1971; Biju-Duval et al., 1968; Boote et al., 1998; Boudjema, 1987; Boumendjel et al., 1988; Carruba et al., 2014; Chavand and Claracq, 1960; Coward and Ries, 2003; Dubois and Mazelet, 1964; Echikh, 1998; Eschard et al., 2010; Fekirine and Abdallah, 1998; Follot, 1950; Frizon de Lamotte et al., 2013; Ghienne et al., 2013; Gindre et al., 2012; Legrand, 1967a, b; Magloire, 1967).

- f. Early Devonian tectonic quiescence (F Fig. 14). This is characterized by a deceleration of the low rate subsidence (DLRS of pattern a, F in Fig. 14). During this period, we have detected Emsian truncation from satellite images (Fig. 6d and e) and erosion and pinch out of Upper Emsian to Eifelian series from well cross sections (Figs. 10, 12 and 13). In previous works, these hiatuses/gaps (i.e., Upper Lochkovian, Lower Pragian,

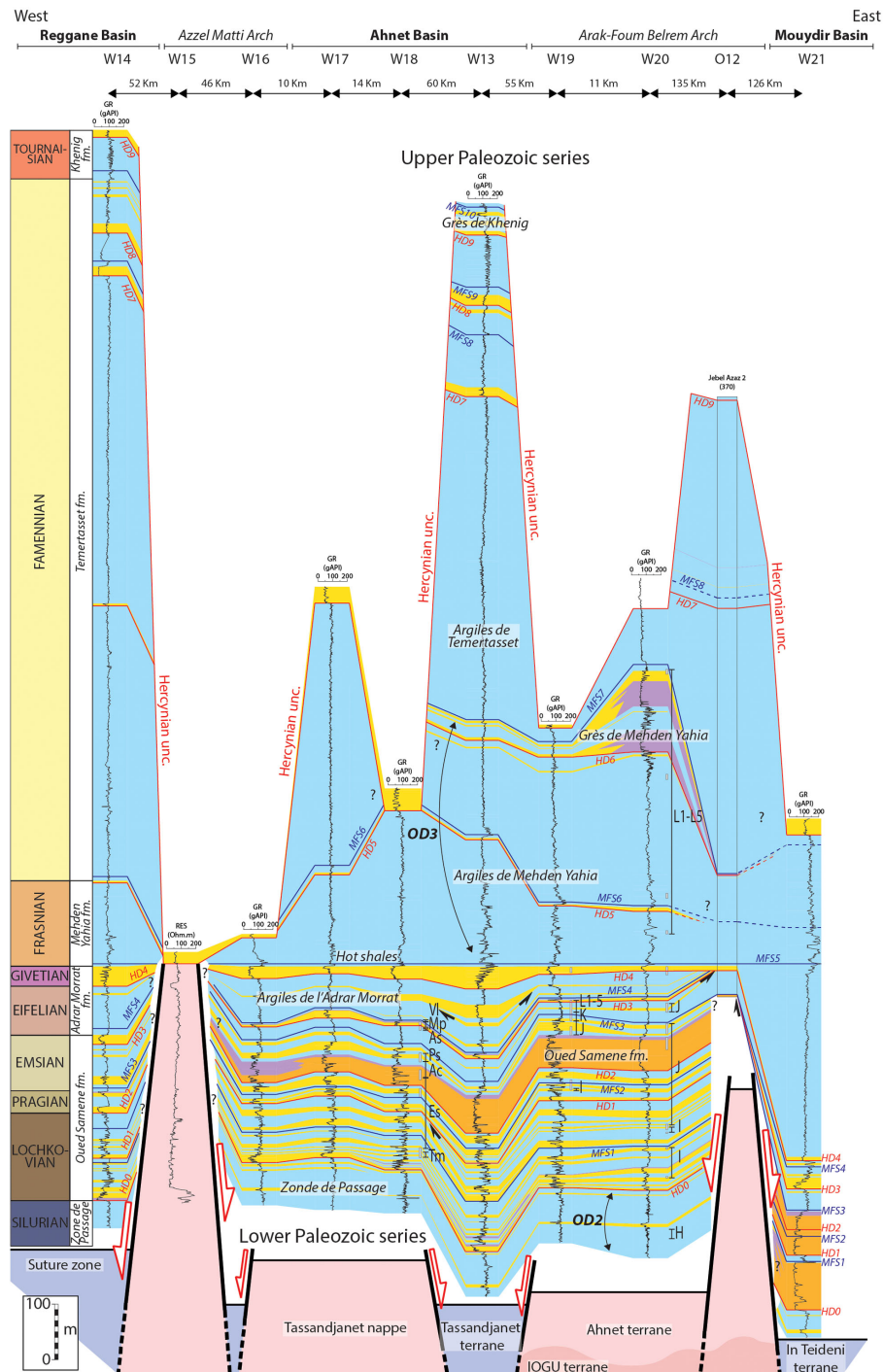


Figure 12. NE–W cross section between the Reggane Basin, the Azzel Matti Arch, the Ahnet Basin, the Arak-Foum Belrem Arch, the Mouydir Basin, and the Amguid El Biod Arch. The well W18 biozone calibration is based on Kermadji et al. (2009): biozone (Tm) *tidikeltense microbaculatus* (Lochkovian, Lower Devonian), biozone (Es) *emsiensis spinaeformis* (Lochkovian–Pragian, Lower Devonian), biozone (Ac) *arenorugosa caperatae* (Pragian, Lower Devonian), biozone (Ps) *poligonalis subgranifer* (Pragian–Emsian, Lower Devonian), biozone (As) *annulatus svalbardiae* (Emsian, Lower Devonian), biozone (Mp) *microancylus protea* (Emsian–Eifelian, Lower to Middle Devonian), and biozone (VI) *velatus langii* (Eifelian, Middle Devonian). The well W19 and W20 biozones calibration from internal reports (Abdesselam-Rouighi, 1991; Khiar, 1974) is based on the Magloire (1967) classification: biozone H (Pridoli, Upper Silurian), biozone I (Lochkovian, Lower Devonian), biozone J (Pragian, Lower Devonian), biozone K (Emsian, Lower Devonian), and biozone L1–5 (Middle Devonian to Upper Devonian). Interpretation of the basement is based on Figs. 1, 2, and 15. Outcrop and well location is in Fig. 2.

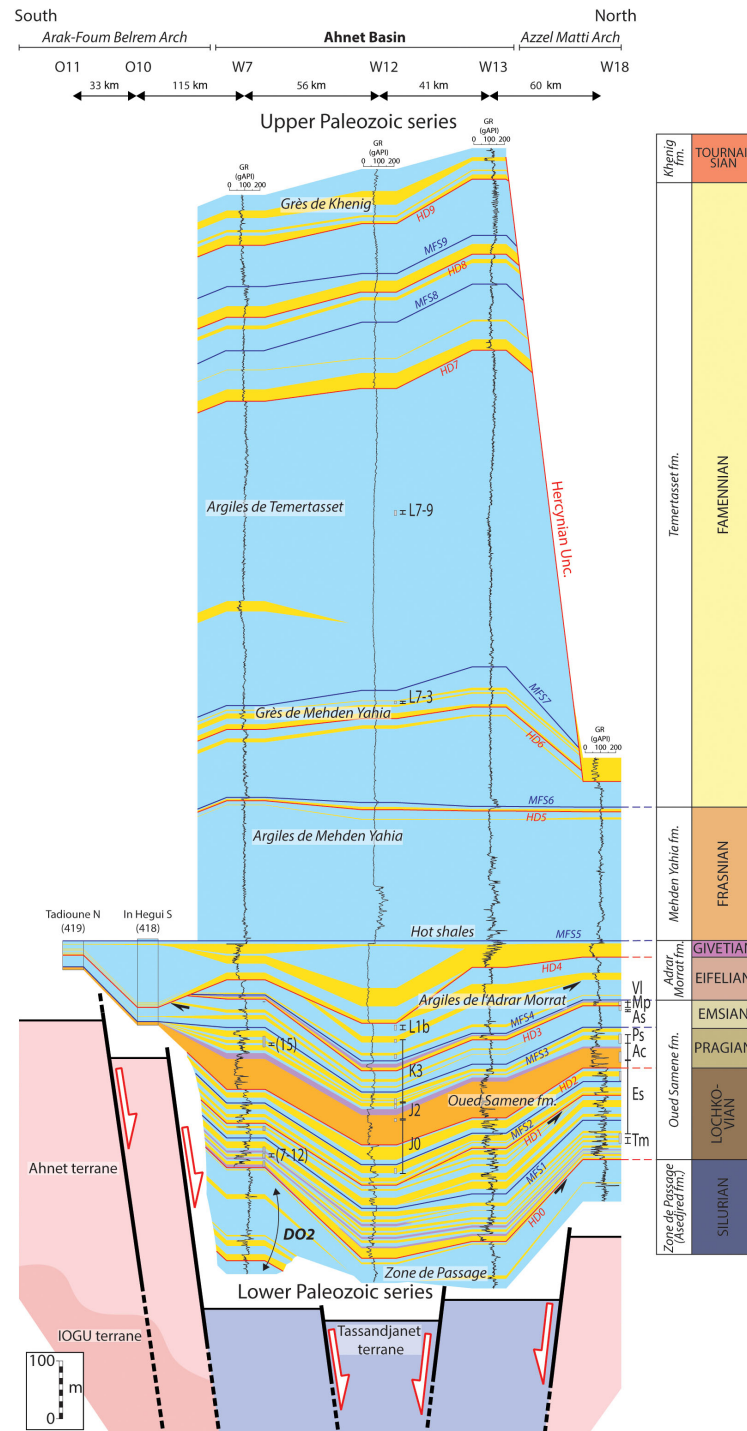


Figure 13. N–S cross section in the Ahnet Basin between Azzel Matti Arch and Arak-Foum Belrem Arch; well W7 biozone calibration from Azzoune, (1999) internal report based on the Boumendjel (1987) classification: biozones 7–12 (Lochkovian, Lower Devonian), biozone 15 (Emsian, Lower Devonian). Well W18 biozone calibration is based on Kermadji et al. (2009): biozone (Tm) *tidikeltense microbaculatus* (Lochkovian, Lower Devonian), biozone (Es) *emsiensis spinaeformis* (Lochkovian–Pragian, Lower Devonian), biozone (Ac) *arenorugosa caperatus* (Pragian, Lower Devonian), biozone (Ps) *polygonalis subgranifer* (Pragian–Emsian, Lower Devonian), biozone (As) *annulatus svalbardiae* (Emsian, Lower Devonian), biozone (Mp) *microancyreus protea* (Emsian–Eifelian, Lower to Middle Devonian), and biozone (VI) *velatus langii* (Eifelian, Middle Devonian). The well W12 biozone calibration from Abdesselam-Rouighi (1977) internal report is based on the Boumendjel (1987) classification: biozone J (Pragian, Lower Devonian), biozone K (Emsian, Lower Devonian), biozone L1 (Eifelian, Middle Devonian), and biozone L7–3, L7–9 (Frasnian–Famennian, Upper Devonian). Interpretation of the basement is based on Figs. 1, 2, and 15. Outcrop and well location is in Fig. 2.

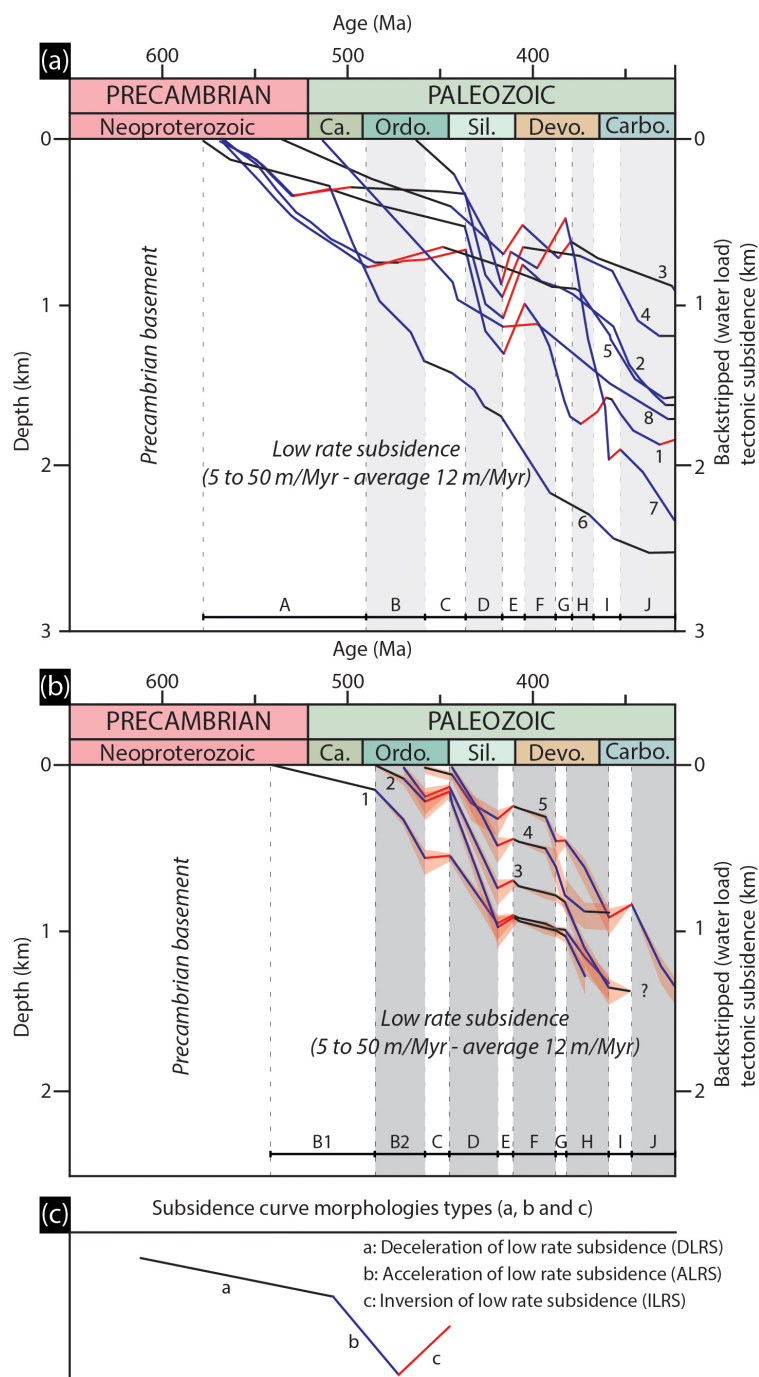


Figure 14. (a) Tectonic backstripped curves of the Paleozoic North Saharan Platform (peri-Hoggar basins) compiled from literature. 1: HAD-1 well in Ghadamès Basin (Makhous and Galushkin, 2003b); 2: well RPL-101 in Reggane Basin (Makhous and Galushkin, 2003b); 3: L1-1 well in Murzuq Basin (Galushkin and Eloghbi, 2014); 4: TGE-1 in Illizi Basin (Makhous and Galushkin, 2003a); 5: REG-1 in Timimoun Basin (Makhous and Galushkin, 2003b); 6: Ghadamès-Berkine Basin (Allen and Armitage, 2011; Yah, 1999); 7: well in Sbâa Basin (Tournier, 2010); and 8: well B1NC43 in Al Kufrah Basin (Holt et al., 2010). (b) Tectonic backstripped curves of wells in the study area 1: well W17 in Ahnet Basin; 2: well W5 in Ahnet Basin; 3: well W7 in Ahnet Basin; 4: well W21 in Mouydir Basin; and 5: well W1 in Reggane Basin. (c) Typologies of subsidence curves morphologies. A: Late Pan-African compression and collapse (type a, b, and c subsidence), B: undifferentiated Cambrian–Ordovician (type a, b, and c subsidence), B1: Cambrian–Ordovician tectonic quiescence (type a subsidence), B2: Cambrian–Ordovician extension (type b subsidence), C: Late Ordovician glacial and isostatic rebound (type c subsidence), D: Silurian extension (type b subsidence), E: Late Silurian Caledonian compression (type c subsidence), F: Early Devonian tectonic quiescence (type a subsidence), G–H: Middle to late Devonian extension with local compression (i.e., inversion structures, type b and c subsidence), I: Early Carboniferous extension with local tectonic pre-Hercynian compression (type c and b subsidence), and J: Middle Carboniferous tectonic extension (type b subsidence).

Upper Pragian, Upper Emsian, Lower Eifelian) are observed in the Ahnet Basin (Kermandji, 2007; Kermandji et al., 2003, 2008, 2009; Wendt et al., 2006), in the Illizi (Boudjema, 1987) and in the Reggane (Jäger et al., 2009).

- g., h. Middle to late Devonian geodynamic pulse (extension and local inversions, G and H Fig. 14). The Middle to Late Devonian period is characterized by large wedge hiatuses and truncations associated with the reactivation of horst and graben structures and local positive inversion (OD3 in Figs. 6d, e, f, 7 and 10 to 13). This period is characterized by inversion and acceleration of low rate subsidence (patterns c and b: ILRS – ALRS, Fig. 14). Some of the Middle to Late Devonian syntectonic structures and hiatuses (e.g., Givetian/Frasnian) are noticed in the Ahnet Basin (Wendt et al., 2006), on the Amguid Ridge (Wendt et al., 2009b), in the Illizi Basin (Boudjema, 1987; Chaumeau et al., 1961; Eschard et al., 2010; Fabre, 2005; Legrand, 1967a), on the Gargaf (Carruba et al., 2014; Collomb, 1962; Fabre, 2005; Massa, 1988) and elsewhere on the platform (Frizon de Lamotte et al., 2013).
- i., j. Pre-Hercynian to Hercynian geodynamic pulses (I and J Fig. 14). This period is organized in Early Carboniferous pre-Hercynian (I, Fig. 14) to Late Carboniferous–Early Permian Hercynian compressions limited by Mid Carboniferous tectonic quiescence/extension (J, Fig. 14). The Carboniferous period is characterized by a normal reactivation and local positive inversion of the previous structural patterns involving reverse faults, overturned folds, transpressional flower structures along strike-slip fault zones (Figs. 6f, 7b, c and d). The major Carboniferous tectonic event on the Saharan Platform impacted all arches and it is mainly controlled by near-vertical basement faults with a strike-slip component (Boote et al., 1998; Caby, 2003; Carruba et al., 2014; Haddoum et al., 2001, 2013; Liégeois et al., 2003; Wendt et al., 2009a; Zazoun, 2001, 2008). According to these authors basement fabric features exerted a very strong control on the structural evolution during the Hercynian deformation. Two major hiatuses (i.e., Mid Tournaisian to Mid Viséan–Serpukhovian) are recognized (Wendt et al., 2009a).

The geodynamic pulses attest to the reactivation of the terranes and associated lithospheric fault zones. This observation questions the nature of the Precambrian basement and associated structural heritage.

7 Basement characterization: Precambrian structural heritage

Geochronological data show that the different terranes were reworked during several main thermo-orogenic events. The

two main events deduced from geochronological data are the Neoproterozoic (i.e., Pan-African) and Paleoproterozoic (i.e., Eburnean) episodes (Bertrand and Caby, 1978). Aeromagnetic anomaly surveys are commonly used to analyze geological features such as rock types and fault zones (e.g., Turner et al., 2007). A similar study was led in the meantime showing similar interpretations (Bournas et al., 2003; Brahimi et al., 2018). In this study, these data highlight the geometries and the extension of the different terranes under the sedimentary cover. Four main domains can be identified from the aeromagnetic anomaly map, delimited by contrasted magnetic signatures and interpreted as suture zones (thick black lines, Fig. 15a). The study area is bounded to the south by the Tuareg Shield (TS), to the north by the south Atlantic Range, to the west by the West African Craton (WAC), and to the east by the East Saharan Craton (ESC) or Saharan Metacraton (Abdelsalam et al., 2002).

The magnetic disturbance features (Fig. 15a) show three main magnetic trends. A major N–S sinuous fabric and two minor sinuous 130–140° E and N45° E trends. The major N–S lineaments coincide with terrane boundaries and mega-shear zones (e.g., 4°50', 4°10', WOSZ, EOSZ, 8°30', RSZ shear zones; Fig. 1). Sigmoidal-shaped terranes 200 to 500 km long and 100 km wide are characterized (red lines in Fig. 15a). The whole assemblage forms a typical SC-shaped shear fabric (Choukroune et al., 1987) associated with vertical mega-shear zones and suture zones (e.g., WOSZ, EOSZ, 4°10', 4°50' or 8°30' Hoggar shear zones in Fig. 1). The SC fabrics combined with subvertical lithospheric shear zones (Fig. 16b and c) are typical features of the Paleoproterozoic accretionary orogens (Cagnard et al., 2011; Chardon et al., 2009). This architecture is concordant with the Neoproterozoic collage of the Tuareg Shield (i.e., mobile belt) between the West African Craton and the East Saharan Craton (i.e., cratonic blocks) described by (Coward and Ries, 2003; Craig et al., 2008).

The gravimetric anomaly map (Fig. 15b) shows a correlation between gravimetric anomalies and tectonic architecture (intracratonic syncline-shaped basin and neighboring arches). Positive anomalies (>66 mGal) are mainly associated with arches, whereas negative anomalies are related to intracratonic basins (<66 mGal). Nevertheless, negative anomaly disturbance is found in the Hoggar Massif probably due to Cenozoic volcanism and the Hoggar swell (Liégeois et al., 2005) or to Eocene Alpine intraplate lithospheric buckling (Rougier et al., 2013).

The Precambrian structural heritage is characterized by accreted lithospheric terranes limited by vertical strike-slip mega-shear zones (Fig. 16b and c). A zonation is observed between the Paleozoic basins and arches configurations and the different terranes (thermo-tectonic age). Arches are linked to Archean to Paleoproterozoic continental terranes in contrast to syncline-shaped basins which are associated with Meso-Neoproterozoic terranes (Figs. 1, 2 and 16a).

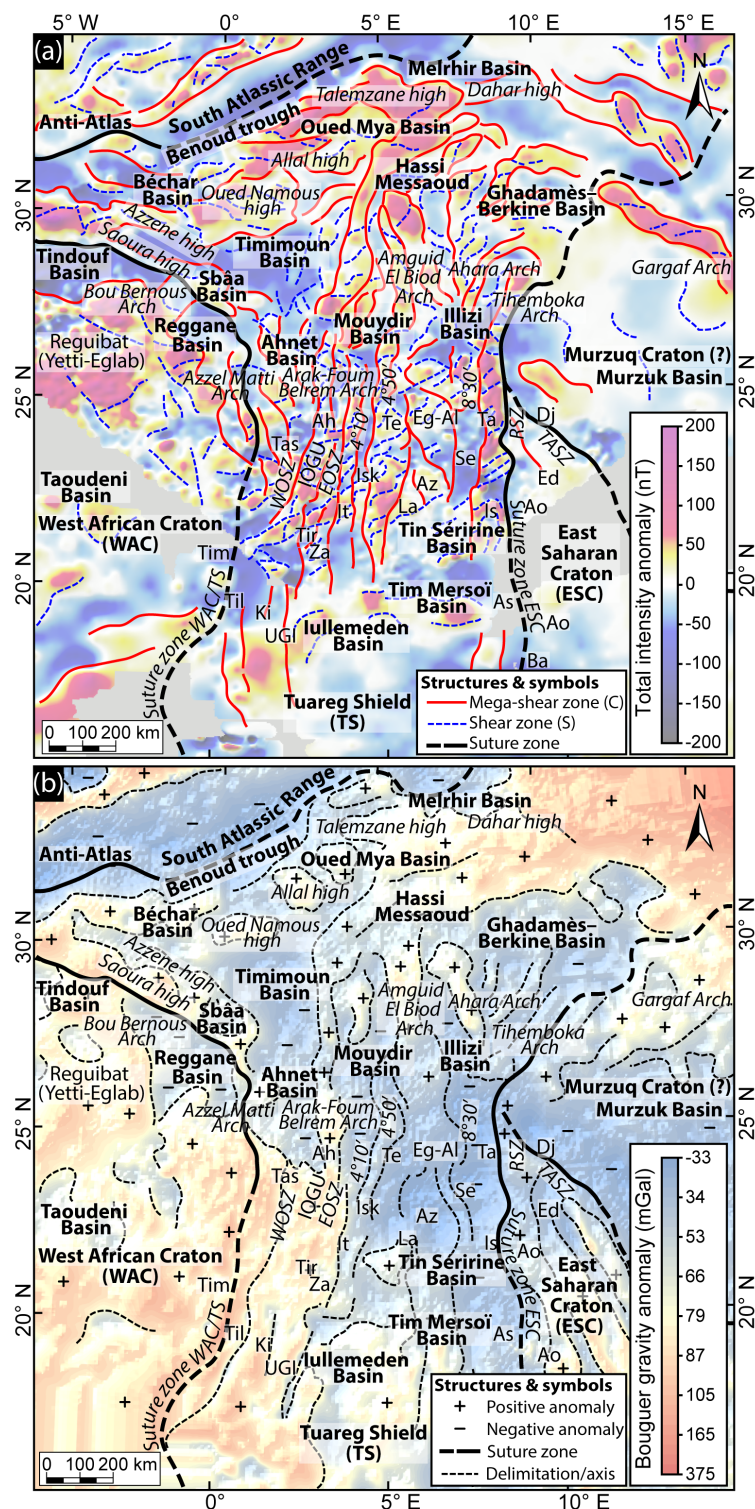


Figure 15. (a) Interpreted aeromagnetic anomaly map (<https://www.geomag.us/>, last access: 1 December 2016) of the Paleozoic North Saharan Platform (peri-Hoggar basins) showing the different terranes delimited by N–S, NW–SE, and NE–SW lineaments and megasigmoid structures (SC – shear fabrics). (b) Bouguer anomaly map (from the International Gravimetric Bureau: <http://bgi.omp.obs-mip.fr/>, last access: 1 December 2016) of the North Saharan Platform (peri-Hoggar basins) presenting evidence of positive anomalies under arches and negative anomalies under basins.

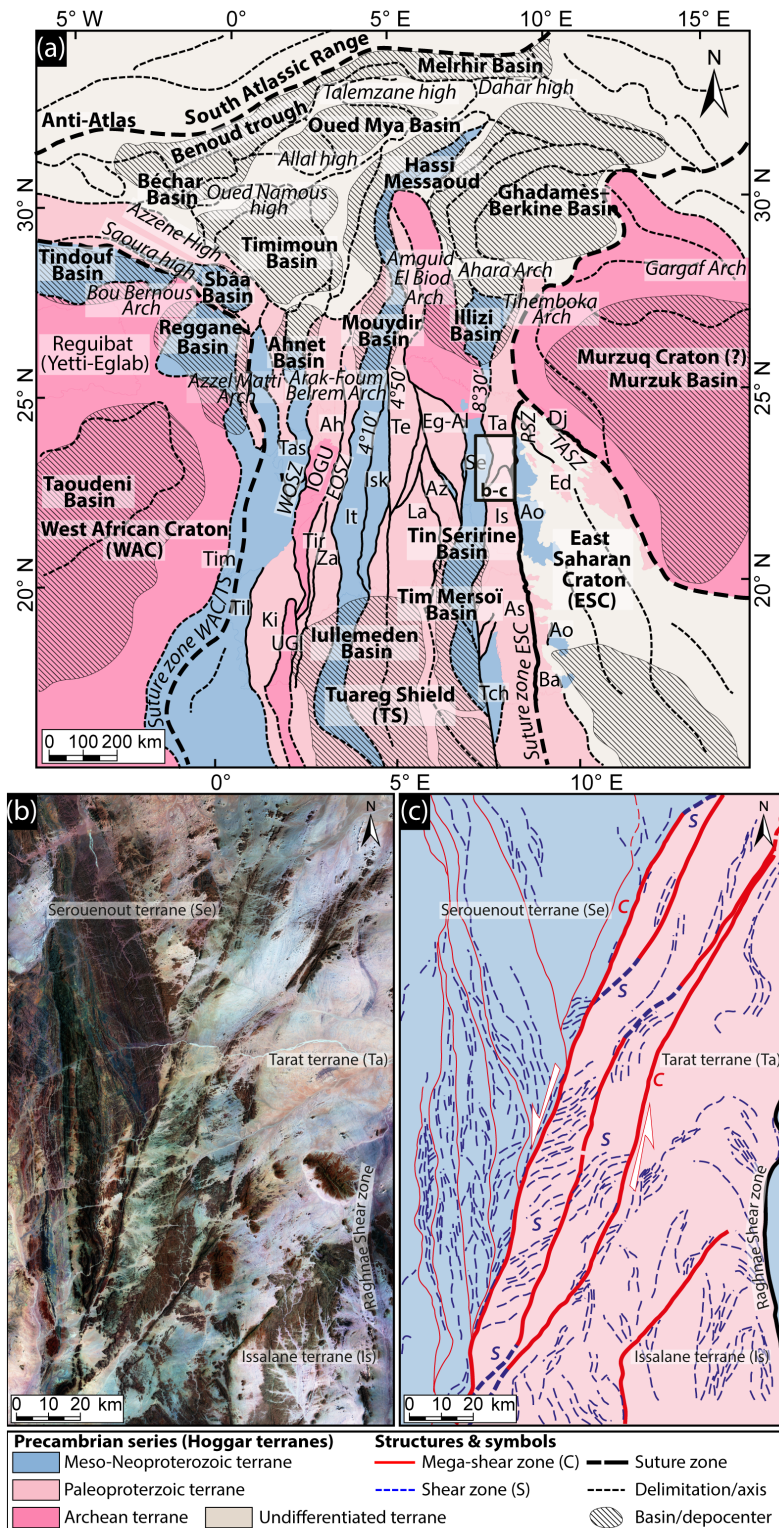


Figure 16. (a) Interpreted map of basement terranes according to their age (compilation of datasets in Fig. 1 and Supplement data 1); (b) Satellite images (7ETM+ from USGS: <https://earthexplorer.usgs.gov/>, last access: 29 October 2016) of Paleoproterozoic Issalane-Tarat terrane, central Hoggar (see C for location). (c) Interpreted satellite images of Paleoproterozoic Issalane-Tarat terrane showing sinistral sigmoid mega-structures associated with transcurrent lithospheric shear fabrics (SC).

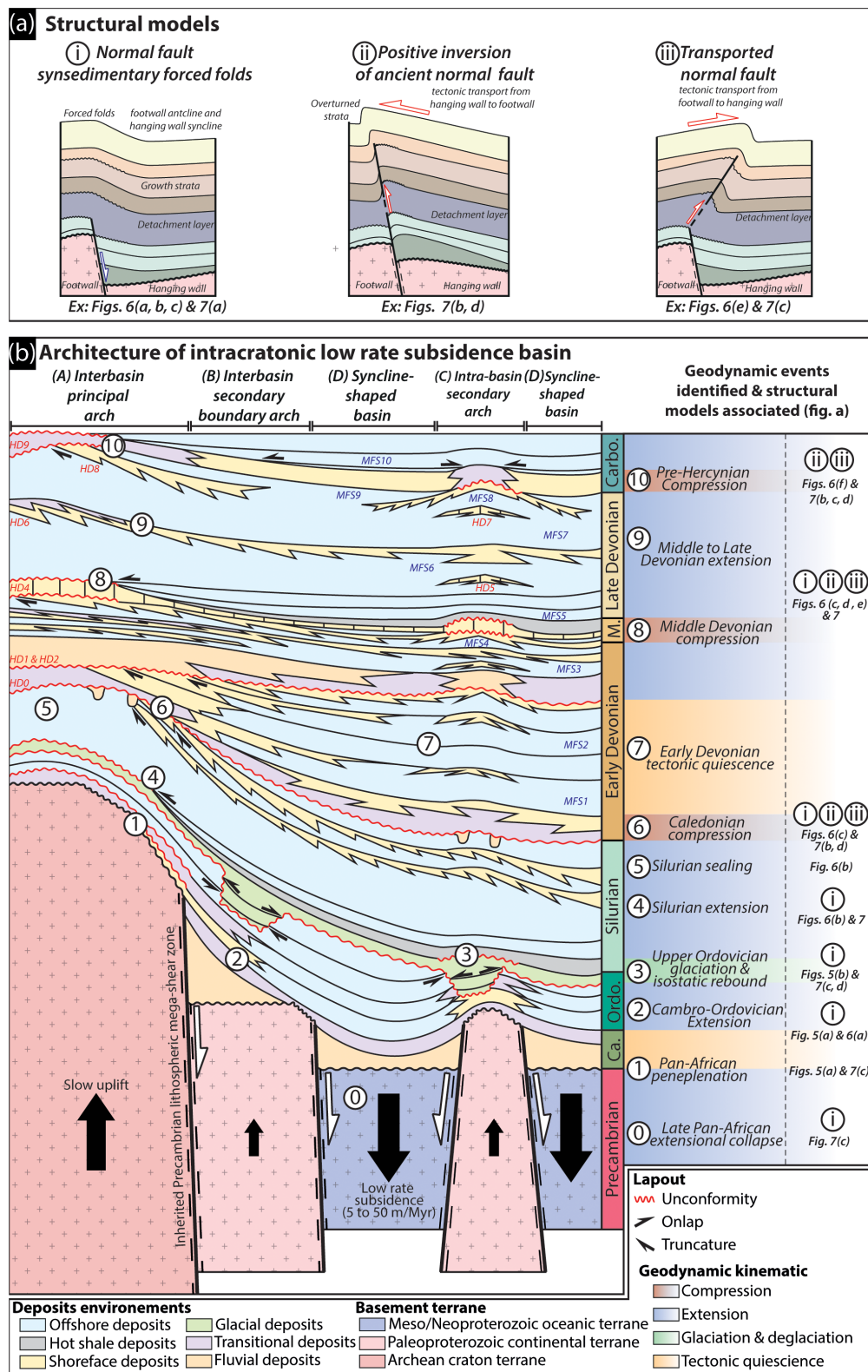


Figure 17. (a) Different structural model styles identified from the analysis of seismic profiles and from interpretation of the satellite images. (b) A conceptual model of the architecture of an intracratonic low rate subsidence basin and synthesis of the tectonic kinematics during the Paleozoic. Note that the differential subsidence between arches and basins is controlled by terrane heterogeneity (i.e., thermo-chronologic age, rheology, etc.).

8 Low subsidence rate intracratonic Paleozoic basins of the central Sahara provide a basis for an integrated modeling study

Paleozoic intracratonic basins with similar characteristics (architecture, subsidence rate, stratigraphic partitioning, alternating episodes of intraplate extension, and short duration compressions with periods of tectonic quiescence, etc.) have been documented in North America (e.g., Allen and Armitage, 2011; Beaumont et al., 1988; Burgess, 2008; Burgess et al., 1997; Eaton and Darbyshire, 2010; Pinet et al., 2013; Potter, 2006; Sloss, 1963; Xie and Heller, 2006), South America (Allen and Armitage, 2011; de Brito Neves et al., 1984; Milani and Zalan, 1999; de Oliveira and Mohriak, 2003; Soares et al., 1978; Zalan et al., 1990), Russia (Allen and Armitage, 2011; Nikishin et al., 1996) and Australia (Harris, 1994; Lindsay and Leven, 1996; Mory et al., 2017). However, the nature of the potential driving processes (lithospheric folding, far-field stresses, local increase in the geotherm, mechanical anisotropy from lithospheric rheological heterogeneity, etc.) associated with the formation of intracratonic Paleozoic basins remains highly speculative (Allen and Armitage, 2011; Armitage and Allen, 2010; Braun et al., 2014; Burgess and Gurnis, 1995; Burov and Cloetingh, 2009; Cacace and Scheck-Wenderoth, 2016; Célérier et al., 2005; Gac et al., 2013; Heine et al., 2008; Leeder, 1991; Vauchez et al., 1998).

The multiscale and multidisciplinary analysis performed in this study enable us to document a model of Paleozoic intracratonic central Saharan basins that couples basin architecture and basement structures (Fig. 17). While we do not provide any quantitative explanations for the dynamics of these basins, our synthesis highlights that their subsidence is not the result of a single process and we attempt to make a check-list here of the properties that a generic model of formation of such basins must capture:

- The association of syncline-shaped wide basins and neighboring arches (i.e., paleo-highs). The structural framework shows a close association of syncline-shaped basins, interbasin principal to secondary arches, and intra-basin secondary arches (see Fig. 2).
- By local horst and graben architecture linked to steep-dipping planar normal faults and associated with normal fault-related fold structures (i.e., forced folds; a, Fig. 17a). Locally, the extensional structures are disrupted by positive inversion structures (b, Fig. 17a) or transported normal faults (c, Fig. 17a).
- A low rate of subsidence ranging between 5 to 50 m Myr⁻¹ (Fig. 14).
- Long periods of extension and tectonic quiescence are interrupted by brief periods of compression or glaciation/deglaciation events (Beuf et al., 1971; Denis et al.,

2007; Le Heron et al., 2006). These periods of compression are possibly related to intraplate compression linked to distal orogenies (i.e., Late Silurian Caledonian event, Late Carboniferous Hercynian, (Frizon de Lamotte et al., 2013) or to intraplate arch uplift related to magmatism (Derder et al., 2016; Fabre, 2005; Frizon de Lamotte et al., 2013; Moreau et al., 1994).

- Synsedimentary divergent onlaps and local unconformities are identified from integrated seismic data, satellite images, and borehole data (Figs. 5, 6, 7 and 10 to 13). The periods of tectonic activity are characterized by normal to reverse reactivation of border faults, emplacement of wedge-shaped units, and erosional unconformities neighboring the arches.
- The stratigraphic architecture displays a lateral facies variation and partitioning between distal marine facies infilling the intracratonic basins (i.e., offshore deposits) and proximal amalgamated facies (i.e., fluvio-marine, shoreface) associated with prominent stratigraphic hiatus and erosional unconformities in the vicinity of the arches.
- A close connection is evidenced between the period of tectonic deformation and the presence of erosional unconformities (i.e., 2, 3, 6, 8, 10 geodynamic events in Fig. 17b). By contrast, the periods of tectonic quiescence and extension are characterized by low lateral facies variations, thin deposits, and the absence of erosional surfaces.
- The Precambrian heritage corresponds to Archean to Paleoproterozoic terranes identified in the Hoggar Massif and reactivated during the Meso-Neoproterozoic Pan-African cycle (Fig. 1). The Precambrian lithospheric heterogeneity illustrated by the different characteristics of Precambrian terranes (wavelength, age, nature, fault zones) spatially control the emplacement of the syncline-shaped intracratonic basins underlain by Meso-Neoproterozoic oceanic terranes and the arches underlain by Archean to Paleoproterozoic continental terranes (Figs. 1, 2 and 16). Many authors suggest control of the basement fabrics is inherited from the Pan-African orogeny in the Saharan basins (Beuf et al., 1968b, 1971; Boote et al., 1998; Carruba et al., 2014; Coward and Ries, 2003; Eschard et al., 2010; Guiraud et al., 2005; Sharata et al., 2015).

9 Conclusions

Our integrated approach using both geophysical (seismic, gravity, aeromagnetic, etc.) and geological (well, seismic, satellite images, etc.) data has enabled us to decrypt the characteristics of the intracratonic Paleozoic Saharan basins and the control of the heterogeneous lithospheric heritage of the

horst and graben architecture, low rate subsidence, and the association of long-lived broad synclines and anticlines (i.e., arches swells, domes, highs or ridges) with very different wavelengths (λ) (tens to hundreds of kilometers). A coupled basin architecture and basement structures model is proposed (Fig. 17).

This study highlights a tight control of the heterogeneous lithosphere zonation over the structuring of the intracratonic central Saharan Basin. This particular type of basin is characterized by a low rate of subsidence and fault activation controlling the homogeneity of sedimentary facies and the distribution of the main unconformities. The low rate activation of vertical mega-shear zones bounding the intracratonic basin during Paleozoic times contrasts markedly with classic rift kinematics and architecture. Three different periods of tectonic compressional pulses (i.e., Caledonian, Middle to Late Devonian, and pre-Hercynian), extension, and quiescence are identified and controlled the sedimentary distribution (Fig. 17). An understanding of tectono-sedimentary interaction is key to understanding the distribution of the Paleozoic petroleum reservoirs of this first-order oil province.

Data availability. Seismic and well log data analysed in this study are part of the Neptune Energy/SONATRACH internal database. Unfortunately, they are not publicly available. Nonetheless, satellite images and geophysical data are all available (see data and methods).

Supplement. The Supplement related to this article is available online at: <https://doi.org/10.5194/se-9-1239-2018-supplement>.

Author contributions. The structural seismic and photogeology interpretation as well as the basement interpretation and analyses throughout this study were mainly undertaken by PP and MG. Interpretations of the well logs, the sedimentology, and the sequence stratigraphy were primarily carried out by PP and EV. Backstripping was led by PP and controlled by IM and EP. The paper was written by PP, with additional input and scientific editing from MG and EV. All authors contributed to the technical interpretation, extensive discussions, and ideas throughout the study and the writing of the paper.

Competing interests. The authors declare that they have no conflict of interest.

Acknowledgements. We are most grateful to Neptune Energy and ENGIE which provided the database used in this paper and funded the work. Special thanks to the data management service of Neptune Energy (especially Aurelie Galvani) for their help with the database. Thanks also go to Jobst Wendt, Réda Samy Zazoun, and

Fabio Lottaroli for detailed reviews/comments, along with a short comment from Alexander Peace, which considerably enriched and improved this paper.

Edited by: Mark Allen

Reviewed by: Reda Samy Zazoun, Fabio Lottaroli, and Jobst Wendt

References

- Abdelsalam, M. G., Liégeois, J.-P., and Stern, R. J.: The saharan metacraton, *J. Afr. Earth Sci.*, 34, 119–136, 2002.
- Abdesselam-Rouighi, F.: Etude palynologique du sondage Sebkhet El Melah (unpublished), Entreprise nationale Sonatrach division hydrocarbures direction Laboratoire central des hydrocarbures, Boumerdès, 1977.
- Abdesselam-Rouighi, F.: Résultats de l'étude palynologiques des sondages Gare El Guefoul Bassin de l'Ahnnet-Mouydir (unpublished), Entreprise nationale Sonatrach division hydrocarbures direction Laboratoire central des hydrocarbures, Boumerdès, 1991.
- Ahmed, A. A.-K. and Moussine-Pouchkine, A.: Lithostratigraphie, sédimentologie et évolution de deux bassins molassiques intramontagneux de la chaîne Pan-Africaine: la Série pourprée de l'Ahnnet, Nord-Ouest du Hoggar, Algérie, *J. Afr. Earth Sci.*, 6, 525–535, 1987.
- Aigner, T.: Storm depositional systems: dynamic stratigraphy in modern and ancient shallow-marine sequences, *Lect. Notes Earth Sci. Berl. Springer Verl.*, 3, 1–158, 1985.
- Allen, J. R. L.: Studies in fluvial sedimentation: bars, bar-complexes and sandstone sheets (low-sinuosity braided streams) in the Brownstones (L. Devonian), Welsh Borders, *Sediment. Geol.*, 33, 237–293, 1983.
- Allen, P. A. and Allen, J. R.: Subsidence and thermal history, in *Basin analysis: Principles and applications*, 349–401, Wiley-Blackwell, Oxford, 2005.
- Allen, P. A. and Armitage, J. J.: Cratonic Basins, in *Tectonics of Sedimentary Basins*, edited by: Busby, C. and Azor, A., 602–620, John Wiley & Sons, Ltd., 2011.
- Angevine, C. L., Heller, P. L., and Paola, C.: Quantitative sedimentary basin modeling, *American Association of Petroleum Geologists*, 1990.
- Armitage, J. J. and Allen, P. A.: Cratonic basins and the long-term subsidence history of continental interiors, *J. Geol. Soc.*, 167, 61–70, <https://doi.org/10.1144/0016-76492009-108>, 2010.
- H. Askri, A. Belmecheri, B. Benrabah, A. Boudjema, K. Boumendjel, M. Daoudi, M. Drid, T. Ghalem, A. M. Docca, H. Ghandriche, A. Ghomari, N. Guellati, M. Khennous, R. Lounici, H. Naili, D. Takherist, and M. Terkmani: Geology of Algeria, in *Well Evaluation Conference Algeria*, 1–93, Schlumberger-Sonatrach., 1995.
- Azzoune, N.: Analyse palynologique de trois (03) échantillons de carottes du sondage W7, Sonatrach (unpublished), Entreprise nationale Sonatrach division hydrocarbures direction Laboratoire central des hydrocarbures, Boumerdès, 1999.
- Badalini, G., Redfern, J., and Carr, I. D.: A synthesis of current understanding of the structural evolution of North Africa, *J. Petrol. Geol.*, 25, 249–258, 2002.

- Beaumont, C., Quinlan, G., and Hamilton, J.: Orogeny and stratigraphy: Numerical models of the Paleozoic in the eastern interior of North America, *Tectonics*, 7, 389–416, 1988.
- Bellahsen, N. and Daniel, J. M.: Fault reactivation control on normal fault growth: an experimental study, *J. Struct. Geol.*, 27, 769–780, <https://doi.org/10.1016/j.jsg.2004.12.003>, 2005.
- Bennacef, A., Beuf, S., Biju-Duval, B., de Charpal, O., Gariel, O., and Rognon, P.: Example of Cratonic Sedimentation: Lower Paleozoic of Algerian Sahara, *AAPG Bull.*, 55, 2225–2245, 1971.
- Bennacef, A., Attar, A., Froukhi, R., Beuf, S., Philippe, G., Schmerber, G., and Vermeire, J. C.: Cartes Géologiques d'Iherir-Dider (NG-32-IX), Iherir (NG-32-X), Illizi (NG-32-XV), Aharhar (NG-32-VIII), Oued Samène (NG-32-XIV), Erg Tihodaine (NG-32-VII), Tin Alkourm (NG-32-V), Djanet (NG-32-IV), Ta-N-Mellet (NG-32-XIII), Ta-N-Elak (NG-32-XIX), Fort Tarat (NG-32-XVI), Tilmas El Mra (NG-31-XXIV), Ers Oum El Lil (NG-31-XXII), Amguid (NG-31-XVIII), 1/200000 Sonatrach-Ministère de l'Industrie et des Mines, Algérie, 1974.
- Bensalah, A., Beuf, S., Gabriel, O., Philippe, G., Lacot, R., Paris, A., Basseto, D., Conrad, J., and Moussine-Pouchkine, A.: Cartes Géologiques de Khanguet El Hadid (NG-31-XVII), Aïn Tidjoubar (NG-31-XVI), Oued Djaret (NG-31-XV), Aoulef El Arab (NG-31-XIV), Reggane (NG-31-XIII), Ifetessene (NG-31-IX), Arak (NG-31-X et NG-31-IV), Meredoua (NG-31-XIII), Tanezrouft (NG-31-VII et NG-31-I), In Heguis (NG-31-IX), Tin Senasset (NG-31-III), Ouallene (NG-31-II) 1/200000 Sonatrach-Ministère de l'Industrie et des Mines, Algérie, 1971.
- Berger, J., Ouzegane, K., Bendaoud, A., Liégeois, J.-P., Kié-nast, J.-R., Bruguier, O., and Caby, R.: Continental subduction recorded by Neoproterozoic eclogite and garnet amphibolites from Western Hoggar (Tassendjanet terrane, Tuareg Shield, Algeria), *Precambrian Res.*, 247, 139–158, <https://doi.org/10.1016/j.precamres.2014.04.002>, 2014.
- Bertrand, J. M. L. and Caby, R.: Geodynamic evolution of the Pan-African orogenic belt: A new interpretation of the Hoggar shield (Algerian Sahara), *Geol. Rundsch.*, 67, 357–388, <https://doi.org/10.1007/BF01802795>, 1978.
- Beuf, S. and Montadert, L.: Géologie-sur une discordance angulaire entre les unités II et III du Cambro-Ordovicien au sud-est de la plaine de Dider (Tassili des Ajjers), *Compte Rendus Hebd. Séances L'Académie Sci.*, 254, 1108–1109, 1962.
- Beuf, S., Biju-Duval, B., Mauvier, A., and Legrand, P.: Nouvelles observations sur le “Cambro-Ordovicien” du Bled El Mass (Sahara central), *Publ. Serv. Géologique Algér. Bull.*, 38, 39–51, 1968a.
- Beuf, S., Biju-Duval, B., De Charpal, O., Gariel, O., Bennacef, A., Black, R., Arene, J., Boissonnas, J., Chachau, F., and Guérangé, B.: Une conséquence directe de la structure du bouclier Africain: L'ébauche des bassins de l'Ahnet et du Mouydir au Paléozoïque inférieur, *Publ. Serv. Géologique L'Algérie Nouv. Sér. Bull.*, 38, 105–134, 1968b.
- Beuf, S., Biju-Duval, B., De Charpal, O., and Gariel, O.: Homogénéité des directions des paléocourants du Dévonien inférieur au Sahara central, *Comptes Rendus L'Académie Sci. Sér. D*, 268, 2026–2029, 1969.
- Beuf, S., Biju-Duval, B., de Charpal, O., Rognon, P., Gabriel, O., and Bennacef, A.: Les grès du Paléozoïque inférieur au Sahara: Sédimentation et discontinuités évolution structurale d'un craton, *Technip*, Paris, 1971.
- Biju-Duval, B., de Charpal, O., Beuf, S., and Bennacef, A.: Lithostratigraphie du Dévonien inférieur dans l'Ahnet et le Mouydir (Sahara Central), *Bull. Serv. Géologique Algérie*, 38, 83–104, 1968.
- Black, R., Latouche, L., Liégeois, J. P., Caby, R., and Bertrand, J. M.: Pan-African displaced terranes in the Tuareg shield (central Sahara), *Geology*, 22, 641–644, 1994.
- Bonini, M., Sani, F., and Antonielli, B.: Basin inversion and contractional reactivation of inherited normal faults: A review based on previous and new experimental models, *Tectonophysics*, 522–523, 55–88, <https://doi.org/10.1016/j.tecto.2011.11.014>, 2012.
- Boote, D. R. D., Clark-Lowes, D. D., and Traut, M. W.: Palaeozoic petroleum systems of North Africa, *Geol. Soc. Lond. Spec. Publ.*, 132, 7–68, <https://doi.org/10.1144/GSL.SP.1998.132.01.02>, 1998.
- Borocco, J. and Nyssen, R.: Nouvelles observations sur les “gres inférieurs” cambro-ordoviciens du Tassili interne (Nord-Hoggar), *Bull. Société Géologique Fr.*, S7-I, 197–206, <https://doi.org/10.2113/gssgfbull.S7-I.2.197>, 1959.
- Boudjema, A.: Evolution structurale du bassin pétrolier “triasique” du Sahara nord oriental (Algérie), *Doctoral dissertation*, Paris 11, France, 1987.
- Boumendjel, K.: Les chitinozoaires du silurien supérieur et du dévonien du Sahara algérien (cadre géologique, systématique, biostratigraphie), *Doctoral dissertation*, Rennes 1, France, 1987.
- Boumendjel, K., Loboziak, S., Paris, F., Steemans, P., and Strel, M.: Biostratigraphie des Miospores et des Chitinozoaires du Silurien supérieur et du Dévonien dans le bassin d'Illizi (S.E. du Sahara algérien), *Geobios*, 21, 329–357, [https://doi.org/10.1016/S0016-6995\(88\)80057-3](https://doi.org/10.1016/S0016-6995(88)80057-3), 1988.
- Bournas, N., Galdeano, A., Hamoudi, M., and Baker, H.: Interpretation of the aeromagnetic map of Eastern Hoggar (Algeria) using the Euler deconvolution, analytic signal and local wavenumber methods, *J. Afr. Earth Sci.*, 37, 191–205, <https://doi.org/10.1016/j.jafrearsci.2002.12.001>, 2003.
- Brahimi, S., Liégeois, J.-P., Ghienne, J.-F., Munsch, M., and Bourmatte, A.: The Tuareg shield terranes revisited and extended towards the northern Gondwana margin: Magnetic and gravimetric constraints, *Earth-Sci. Rev.*, 185, 572–599, <https://doi.org/10.1016/j.earscirev.2018.07.002>, 2018.
- Braun, J., Simon-Labric, T., Murray, K. E., and Reinert, P. W.: Topographic relief driven by variations in surface rock density, *Nat. Geosci.*, 7, 534–540, <https://doi.org/10.1038/ngeo2171>, 2014.
- Buchanan, P. G. and McClay, K. R.: Sandbox experiments of inverted listric and planar fault systems, *Tectonophysics*, 188, 97–115, [https://doi.org/10.1016/0040-1951\(91\)90317-L](https://doi.org/10.1016/0040-1951(91)90317-L), 1991.
- Burgess, P. M.: Phanerozoic evolution of the sedimentary cover of the North American craton, in: *Sedimentary Basins of the World*, 5, 31–63, Elsevier, 2008.
- Burgess, P. M. and Gurnis, M.: Mechanisms for the formation of cratonic stratigraphic sequences, *Earth Planet. Sc. Lett.*, 136, 647–663, [https://doi.org/10.1016/0012-821X\(95\)00204-P](https://doi.org/10.1016/0012-821X(95)00204-P), 1995.
- Burgess, P. M., Gurnis, M., and Moresi, L.: Formation of sequences in the cratonic interior of North America by interaction between mantle, eustatic, and stratigraphic processes, *Geol. Soc. Am. Bull.*, 109, 1515–1535, 1997.
- Burke, K., MacGregor, D. S., and Cameron, N. R.: Africa's petroleum systems: four tectonic “Aces” in the past 600 million years, *Geol. Soc. Lond. Spec. Publ.*, 207, 21–60, 2003.

- Burov, E. and Cloetingh, S.: Controls of mantle plumes and lithospheric folding on modes of intraplate continental tectonics: differences and similarities, *Geophys. J. Int.*, 178, 1691–1722, <https://doi.org/10.1111/j.1365-246X.2009.04238.x>, 2009.
- Butler, R. W. H.: The influence of pre-existing basin structure on thrust system evolution in the Western Alps, *Geol. Soc. Lond. Spec. Publ.*, 44, 105–122, <https://doi.org/10.1144/GSL.SP.1989.044.01.07>, 1989.
- Caby, R.: Terrane assembly and geodynamic evolution of central–western Hoggar: a synthesis, *J. Afr. Earth Sci.*, 37, 133–159, <https://doi.org/10.1016/j.jafrearsci.2003.05.003>, 2003.
- Cacace, M. and Scheck-Wenderoth, M.: Why intracontinental basins subside longer: 3-D feedback effects of lithospheric cooling and sedimentation on the flexural strength of the lithosphere: Subsidence at Intracontinental Basins, *J. Geophys. Res.-Sol. Ea.*, 121, 3742–3761, <https://doi.org/10.1002/2015JB012682>, 2016.
- Cagnard, F., Barbey, P., and Gapais, D.: Transition between “Archaean-type” and “modern-type” tectonics: Insights from the Finnish Lapland Granulite Belt, *Precambrian Res.*, 187, 127–142, <https://doi.org/10.1016/j.precamres.2011.02.007>, 2011.
- Carr, I. D.: Second-Order Sequence Stratigraphy of the Palaeozoic of North Africa, *J. Petrol. Geol.*, 25, 259–280, <https://doi.org/10.1111/j.1747-5457.2002.tb00009.x>, 2002.
- Carruba, S., Perotti, C., Rinaldi, M., Bresciani, I., and Bertozzi, G.: Intraplate deformation of the Al Qarqaf Arch and the southern sector of the Ghadames Basin (SW Libya), *J. Afr. Earth Sci.*, 97, 19–39, <https://doi.org/10.1016/j.jafrearsci.2014.05.001>, 2014.
- Catuneanu, O., Abreu, V., Bhattacharya, J. P., Blum, M. D., Dalrymple, R. W., Eriksson, P. G., Fielding, C. R., Fisher, W. L., Galloway, W. E., Gibling, M. R., Giles, K. A., Holbrook, J. M., Jordan, R., Kendall, C. G. S. C., Macurda, B., Martinsen, O. J., Miall, A. D., Neal, J. E., Nummedal, D., Pomar, L., Posamentier, H. W., Pratt, B. R., Sarg, J. F., Shanley, K. W., Steel, R. J., Strasser, A., Tucker, M. E., and Winker, C.: Towards the standardization of sequence stratigraphy, *Earth-Sci. Rev.*, 92, 1–33, <https://doi.org/10.1016/j.earscirev.2008.10.003>, 2009.
- Célériér, J., Sandiford, M., Hansen, D. L., and Quigley, M.: Modes of active intraplate deformation, Flinders Ranges, Australia, *Tectonics*, 24, 1–17, <https://doi.org/10.1029/2004TC001679>, 2005.
- Chardon, D., Gapais, D., and Cagnard, F.: Flow of ultra-hot orogens: A view from the Precambrian, clues for the Phanerozoic, *Tectonophysics*, 477, 105–118, <https://doi.org/10.1016/j.tecto.2009.03.008>, 2009.
- Chaumeau, J., Legrand, P., and Renaud, A.: Contribution à l'étude du Couvinien dans le bassin de Fort-de-Polignac (Sahara), *Bull. Société Géologique Fr.*, S7-III, 449–456, <https://doi.org/10.2113/gssgfbull.S7-III.5.449>, 1961.
- Chavand, J. C. and Claracq, P.: La disparition du Tassili externe à l'E de Fort-Polignac (Sahara central), *CR Soc Géol Fr*, 1959, 172–174, 1960.
- Choukroune, P., Gapais, D., and Merle, O.: Shear criteria and structural symmetry, *J. Struct. Geol.*, 9, 525–530, [https://doi.org/10.1016/0191-8141\(87\)90137-4](https://doi.org/10.1016/0191-8141(87)90137-4), 1987.
- Claracq, P., Fabre, C., Freulon, J. M., and Nougarede, F.: Une discordance angulaire dans les “Grès inférieurs” de l'Adrar Tan Elak (Sahara central), *C. r. Somm. Séances Soc. Géologique Fr.*, 309–310, 1958.
- Collomb, G. R.: Étude géologique du Jebel Fezzan et de sa bordure paléozoïque, Compagnie française des pétroles, 1962.
- Conrad, J.: Les grandes lignes stratigraphiques et sédimentologiques du Carbonifère de l'Ahnnet-Mouydir (Sahara central algérien), *Rev. Inst. Fr. Pétrole*, 28, 3–18, 1973.
- Conrad, J.: Les séries carbonifères du Sahara central algérien: stratigraphie, sédimentation, évolution structurale, Doctoral dissertation, Université Aix-Marseille III, France, 1984.
- Coward, M. P. and Ries, A. C.: Tectonic development of North African basins, *Geol. Soc. Lond. Spec. Publ.*, 207, 61–83, <https://doi.org/10.1144/GSL.SP.2003.207.4>, 2003.
- Cózar, P., Somerville, I. D., Vachard, D., Coronado, I., García-Frank, A., Medina-Varea, P., Said, I., Del Moral, B., and Rodríguez, S.: Upper Mississippian to lower Pennsylvanian biostratigraphic correlation of the Sahara Platform successions on the northern margin of Gondwana (Morocco, Algeria, Libya), *Gondwana Res.*, 36, 459–472, <https://doi.org/10.1016/j.gr.2015.07.019>, 2016.
- Craig, J., Rizzi, C., Said, F., Thusu, B., Luning, S., Asbali, A. I., Keeley, M. L., Bell, J. F., Durham, M. J., and Eales, M. H.: Structural styles and prospectivity in the Precambrian and Palaeozoic hydrocarbon systems of North Africa, *Geol. East Libya*, 4, 51–122, 2008.
- Dalrymple, R. W. and Choi, K.: Morphologic and facies trends through the fluvial–marine transition in tide-dominated depositional systems: A schematic framework for environmental and sequence-stratigraphic interpretation, *Earth-Sci. Rev.*, 81, 135–174, <https://doi.org/10.1016/j.earscirev.2006.10.002>, 2007.
- Dalrymple, R. W., Zaitlin, B. A., and Boyd, R.: A conceptual model of estuarine sedimentation, *J. Sediment. Petrol.*, 62, 1130–1146, 1992.
- Dalrymple, R. W., Mackay, D. A., Ichaso, A. A., and Choi, K. S.: Processes, Morphodynamics, and Facies of Tide-Dominated Estuaries, in *Principles of Tidal Sedimentology*, 79–107, Springer, Dordrecht, 2012.
- de Brito Neves, B. B., Fuck, R. A., Cordani, U. G., and Thomaz, F. A.: Influence of basement structures on the evolution of the major sedimentary basins of Brazil: A case of tectonic heritage, *J. Geodyn.*, 1, 495–510, [https://doi.org/10.1016/0264-3707\(84\)90021-8](https://doi.org/10.1016/0264-3707(84)90021-8), 1984.
- Denis, M., Buoncristiani, J.-F., Konaté, M., Ghienne, J.-F., and Guiraud, M.: Hirnantian glacial and deglacial record in SW Djado Basin (NE Niger), *Geodin. Acta*, 20, 177–195, <https://doi.org/10.3166/ga.20.177-195>, 2007.
- de Oliveira, D. C. and Mohriak, W. U.: Jaibaras trough: an important element in the early tectonic evolution of the Parnaíba interior sag basin, Northern Brazil, *Mar. Petrol. Geol.*, 20, 351–383, [https://doi.org/10.1016/S0264-8172\(03\)00044-8](https://doi.org/10.1016/S0264-8172(03)00044-8), 2003.
- Derder, M. E. M., Maouche, S., Liégeois, J. P., Henry, B., Amenna, M., Ouabadi, A., Bellon, H., Bruguier, O., Bayou, B., Bestandji, R., Nouar, O., Bouabdallah, H., Ayache, M., and Beddiaf, M.: Discovery of a Devonian mafic magmatism on the western border of the Murzuq basin (Saharan metacraton): Paleomagnetic dating and geodynamical implications, *J. Afr. Earth Sci.*, 115, 159–176, <https://doi.org/10.1016/j.jafrearsci.2015.11.019>, 2016.
- Djouder, H., Luning, S., Da Silva, A.-C., Abdallah, H., and Boulvain, F.: Silurian deltaic progradation, Tassili n'Ajjer plateau, south-eastern Algeria: Sedimentology, ichnology and sequence stratigraphy, *J. Afr. Earth Sci.*, 142, 170–192, 2018.
- Dokka, A. M.: Sedimentological core description WELL: W7, Block – 340, (District – 3) (unpublished), Core description,

- Sonatrach division exploration direction des opérations département assistance aux opérations service géologique, Algérie, 1999.
- Dott, R. H. and Bourgeois, J.: Hummocky stratification: Significance of its variable bedding sequences, *Geol. Soc. Am. Bull.*, 93, 663–680, [https://doi.org/10.1130/0016-7606\(1982\)93<663:HSSOIV>2.0.CO;2](https://doi.org/10.1130/0016-7606(1982)93<663:HSSOIV>2.0.CO;2), 1982.
- Dubois, P.: Stratigraphie du Cambro-Ordovicien du Tassili n'Ajjer (Sahara central), *Bull. Société Géologique Fr.*, S7-III, 206–209, <https://doi.org/10.2113/gssgfbull.S7-III.2.206>, 1961.
- Dubois, P. and Mazelet, P.: Stratigraphie du Silurien du Tassili N'Ajjer, *Bull. Société Géologique Fr.*, S7-VI, 586–591, <https://doi.org/10.2113/gssgfbull.S7-VI.4.586>, 1964.
- Dubois, P., Beuf, S., and Biju-Duval, B.: Lithostratigraphie du Dévonien inférieur gréseux du Tassili n'Ajjer, in *Symposium on the Lower Devonian and its limits: Bur. Recherche Geol. et Minieres Mem.*, 227–235, 1967.
- Dumas, S. and Arnott, R. W. C.: Origin of hummocky and swaley cross-stratification – the controlling influence of unidirectional current strength and aggradation rate, *Geology*, 34, 1073–1076, 2006.
- Eaton, D. W. and Darbyshire, F.: Lithospheric architecture and tectonic evolution of the Hudson Bay region, *Tectonophysics*, 480, 1–22, <https://doi.org/10.1016/j.tecto.2009.09.006>, 2010.
- Echikh, K.: Geology and hydrocarbon occurrences in the Ghadames basin, Algeria, Tunisia, Libya, *Geol. Soc. Lond. Spec. Publ.*, 132, 109–129, 1998.
- Eschard, R., Desaubliaux, G., Deschamps, R., Montadert, L., Ravenne, C., Bekkouche, D., Abdallah, H., Belhaouas, S., Benkouider, M., Braik, F., Henniche, M., Maache, N., and Mouaici, R.: Illizi-Berkine Devonian Reservoir Consortium (unpublished), Institut Française du Pétrole – Sontrach, Algérie, 1999.
- Eschard, R., Abdallah, H., Braik, F., and Desaubliaux, G.: The Lower Paleozoic succession in the Tassili outcrops, Algeria: sedimentology and sequence stratigraphy, *First Break*, 23, 27–36, 2005.
- Eschard, R., Braik, F., Bekkouche, D., Rahuma, M. B., Desaubliaux, G., Deschamps, R., and Proust, J. N.: Palaeohighs: their influence on the North African Palaeozoic petroleum systems, *Pet. Geol. Mature Basins New Front. 7th Pet. Geol. Conf.*, 707–724, 2010.
- Fabre, J.: Les séries paléozoïques d'Afrique: une approche, *J. Afr. Earth Sci. Middle East*, 7, 1–40, [https://doi.org/10.1016/0899-5362\(88\)90051-6](https://doi.org/10.1016/0899-5362(88)90051-6), 1988.
- Fabre, J.: Géologie du Sahara occidental et central, Musée royal de l'Afrique centrale, 2005.
- Fabre, J., Kaci, A. A., Bouima, T., and Moussine-Pouchkine, A.: Le cycle molassique dans le Rameau trans-saharien de la chaîne panafricaine, *J. Afr. Earth Sci.*, 7, 41–55, [https://doi.org/10.1016/0899-5362\(88\)90052-8](https://doi.org/10.1016/0899-5362(88)90052-8), 1988.
- Fekirine, B. and Abdallah, H.: Palaeozoic lithofacies correlates and sequence stratigraphy of the Saharan Platform, Algeria, *Geol. Soc. Lond. Spec. Publ.*, 132, 97–108, <https://doi.org/10.1144/GSL.SP.1998.132.01.05>, 1998.
- Fezaa, N., Liégeois, J.-P., Abdallah, N., Cherfouh, E. H., De Waele, B., Bruguier, O., and Ouabadi, A.: Late Ediacaran geological evolution (575–555Ma) of the Djanet Terrane, Eastern Hoggar, Algeria, evidence for a Murzukian intracontinental episode, *Precambrian Res.*, 180, 299–327, <https://doi.org/10.1016/j.precamres.2010.05.011>, 2010.
- Follot, J.: Sur l'existence de mouvements calédoniens au Mouydir (Sahara Central), *Compte Rendus Hebd. Séances L'Académie Sci.*, 230, 2217–2218, 1950.
- Frey, R. W., Pemberton, S. G., and Saunders, T. D.: Ichnofacies and bathymetry: a passive relationship, *J. Paleontol.*, 64, 155–158, 1990.
- Frizon de Lamotte, D., Tavakoli-Shirazi, S., Leturmy, P., Averbuch, O., Mouchot, N., Raulin, C., Leparmentier, F., Blanpied, C., and Ringenbach, J.-C.: Evidence for Late Devonian vertical movements and extensional deformation in northern Africa and Arabia: Integration in the geodynamics of the Devonian world: Devonian evolution Northern Gondwana, *Tectonics*, 32, 107–122, <https://doi.org/10.1002/tect.20007>, 2013.
- Fröhlich, S., Petitpierre, L., Redfern, J., Grech, P., Bodin, S., and Lang, S.: Sedimentological and sequence stratigraphic analysis of Carboniferous deposits in western Libya: Recording the sedimentary response of the northern Gondwana margin to climate and sea-level changes, *J. Afr. Earth Sci.*, 57, 279–296, <https://doi.org/10.1016/j.jafrearsci.2009.09.007>, 2010.
- Gac, S., Huismans, R. S., Simon, N. S. C., Podladchikov, Y. Y., and Faleide, J. I.: Formation of intracratonic basins by lithospheric shortening and phase changes: a case study from the ultra-deep East Barents Sea basin, *Terra Nova*, 25, 459–464, <https://doi.org/10.1111/ter.12057>, 2013.
- Galeazzi, S., Point, O., Haddadi, N., Mather, J., and Druésne, D.: Regional geology and petroleum systems of the Illizi-Berkine area of the Algerian Saharan Platform: An overview, *Mar. Petrol. Geol.*, 27, 143–178, <https://doi.org/10.1016/j.marpetgeo.2008.10.002>, 2010.
- Galloway, W. E.: Genetic Stratigraphic Sequences in Basin Analysis I: Architecture and Genesis of Flooding-Surface Bounded Depositional Units, *AAPG Bull.*, 73, 125–142, 1989.
- Galushkin, Y. I. and Eloghbi, S.: Thermal history of the Murzuq Basin, Libya, and generation of hydrocarbons in its source rocks, *Geochem. Int.*, 52, 486–499, <https://doi.org/10.1134/S0016702914060032>, 2014.
- Gariel, O., de Charpal, O., and Bennacef, A.: Sur la sédimentation des gres du Cambro-Ordovicien (Unité II) dans l'Ahnnet et le Mouydir (Sahara central): Algérie, *Serv. Geol. Bull. N Ser.*, 38, 7–37, 1968.
- Ghienne, J.-F., Deynoux, M., Manatschal, G., and Rubino, J.-L.: Palaeovalleys and fault-controlled depocentres in the Late-Ordovician glacial record of the Murzuq Basin (central Libya), *C. R. Geosci.*, 335, 1091–1100, <https://doi.org/10.1016/j.crte.2003.09.010>, 2003.
- Ghienne, J.-F., Moreau, J., Degermann, L., and Rubino, J.-L.: Lower Palaeozoic unconformities in an intracratonic platform setting: glacial erosion versus tectonics in the eastern Murzuq Basin (southern Libya), *Int. J. Earth Sci.*, 102, 455–482, <https://doi.org/10.1007/s00531-012-0815-y>, 2013.
- Gindre, L., Le Heron, D., and Bjørnseth, H. M.: High resolution facies analysis and sequence stratigraphy of the Siluro-Devonian succession of Al Kufrah basin (SE Libya), *J. Afr. Earth Sci.*, 76, 8–26, <https://doi.org/10.1016/j.jafrearsci.2012.08.002>, 2012.
- Girard, F., Ghienne, J.-F., and Rubino, J.-L.: Channelized sandstone bodies (“cordons”) in the Tassili N'Ajjer (Algeria & Libya): snapshots of a Late Ordovician proglacial out-

- wash plain, *Geol. Soc. Lond. Spec. Publ.*, 368, 355–379, <https://doi.org/10.1144/SP368.3>, 2012.
- Grasemann, B., Martel, S., and Passchier, C.: Reverse and normal drag along a fault, *J. Struct. Geol.*, 27, 999–1010, <https://doi.org/10.1016/j.jsg.2005.04.006>, 2005.
- Greigert, J. and Pognet, R.: Carte Géologique du Niger, 1/2000000, BRGM, République du Niger, 1965.
- Guiraud, R., Bosworth, W., Thierry, J., and Delplanque, A.: Phanerozoic geological evolution of Northern and Central Africa: An overview, *J. Afr. Earth Sci.*, 43, 83–143, <https://doi.org/10.1016/j.jafrearsci.2005.07.017>, 2005.
- Haddoum, H., Guiraud, R., and Moussine-Pouchkine, A.: Hercynian compressional deformations of the Ahnet–Mouydir Basin, Algerian Saharan Platform: far-field stress effects of the Late Palaeozoic orogeny, *Terra Nova*, 13, 220–226, 2001.
- Haddoum, H., Mokri, M., Ouzegane, K., Ait-Djaffer, S., and Djemai, S.: Extrusion de l'In Ouzal vers le Nord (Hoggar occidental, Algérie): une conséquence d'un poinçonnement panafricain, *J. Hydrocarb. Mines Environ. Res. Vol.*, 4, 6–16, 2013.
- Haq, B. U. and Schutter, S. R.: A Chronology of Paleozoic Sea-Level Changes, *Science*, 322, 64–68, <https://doi.org/10.1126/science.1161648>, 2008.
- Harris, L. B.: Structural and tectonic synthesis for the Perth basin, Western Australia, *J. Petrol. Geol.*, 17, 129–156, 1994.
- Hartley, R. W. and Allen, P. A.: Interior cratonic basins of Africa: relation to continental break-up and role of mantle convection, *Basin Res.*, 6, 95–113, 1994.
- Hassan, A.: Etude palynologique Paléozoïque du sondage Razzal-Allah-Nord (unpublished), Entreprise nationale Sonatrach division hydrocarbures direction Laboratoire central des hydrocarbures, Boumerdès, 1984.
- Heine, C., Dietmar Müller, R., Steinberger, B., and Torsvik, T. H.: Subsidence in intracontinental basins due to dynamic topography, *Phys. Earth Planet. Int.*, 171, 252–264, <https://doi.org/10.1016/j.pepi.2008.05.008>, 2008.
- Henniche, M.: Architecture et modèle de dépôts d'une série sédimentaire paléozoïque en contexte cratonique, Rennes 1, France, 2002.
- Holbrook, J. and Schumm, S. A.: Geomorphic and sedimentary response of rivers to tectonic deformation: a brief review and critique of a tool for recognizing subtle epeirogenic deformation in modern and ancient settings, *Tectonophysics*, 305, 287–306, 1999.
- Hollard, H., Choubert, G., Bronner, G., Marchand, J., and Sougy, J.: Carte géologique du Maroc, scale 1: 1 000 000, Serv. Carte Géol. Maroc., 260, 1985.
- Holt, P. J., Allen, M. B., van Hunen, J., and Bjørnseth, H. M.: Lithospheric cooling and thickening as a basin forming mechanism, *Tectonophysics*, 495, 184–194, <https://doi.org/10.1016/j.tecto.2010.09.014>, 2010.
- Jacquemont, P., Jutard, G., Plauchut, B., Grégoire, J., and Mouflard, R.: Etude du bassin du Djado, *Bur. Rech. Pétroles Rapp.*, 1215, 1959.
- Jäger, H., Lewandowski, E., and Lampart, V.: Palynology of the upper Silurian to middle Devonian in the Reggane Basin, southern Algeria, *Ext. Abstr. DGMK-Tagungsbericht 2009-1 DGMKÖGEW Spring Meet. Celle*, 47–51, 2009.
- Jardiné, S. and Yapaudjian, L.: Lithostratigraphie et palynologie du Dévonien-Gothlandien gréseux du Bassin de Polignac (Sahara), *Rev. L'Institut Fr. Pétrole*, 23, 439–469, 1968.
- Joulié, F.: Carte géologique de reconnaissance de la bordure sédimentaire occidentale de l'Aïr au 1/500 000, Éditions BRGM Orléans Fr., 1963.
- Kermadji, A. M.: Silurian–Devonian miospores from the western and central Algeria, *Rev. Micropaléontol.*, 50, 109–128, <https://doi.org/10.1016/j.revmic.2007.01.003>, 2007.
- Kermadji, A. M. H., Kowalski, M. W., and Pharissat, A.: Palynologie et séquences de l'Emsien de la région d'In Salah, Sahara central Algérien, *Bull. Société D'Histoire Nat. Pays Montbél.*, 301–306, 2003.
- Kermadji, A. M. H., Kowalski, W. M., and Touhami, F. K.: Miospore stratigraphy of Lower and early Middle Devonian deposits from Tidikelt, Central Sahara, Algeria, *Geobios*, 41, 227–251, <https://doi.org/10.1016/j.geobios.2007.05.002>, 2008.
- Kermadji, A. M. H., Touhami, F. K., Kowalski, W. M., Abbès, S. B., Boularak, M., Chabour, N., Laifa, E. L., and Hannachi, H. B.: Stratigraphie du Dévonien Inférieur du Plateau du Tidikelt d'In Salah (Sahara Central Algérie), *Comun. Geológicas*, 96, 67–82, 2009.
- Khalil, S. M. and McClay, K. R.: Extensional fault-related folding, northwestern Red Sea, Egypt, *J. Struct. Geol.*, 24, 743–762, 2002.
- Khier, S.: Résultats palynologiques du sondage Garet El Guefoul (unpublished), Entreprise nationale Sonatrach division hydrocarbures direction Laboratoire central des hydrocarbures, Alger, 1974.
- Kracha, N.: Relation entre sédimentologie, fracturation naturelle et diagénèse d'un réservoir à faible perméabilité application aux réservoirs de l'Ordovicien bassin de l'Ahnet, Sahara central, Algérie, Doctoral dissertation, Université des sciences et technologies de Lille, France, 2011.
- Le Heron, D. P.: Interpretation of Late Ordovician glaciogenic reservoirs from 3-D seismic data: an example from the Murzuq Basin, Libya, *Geol. Mag.*, 147, 28–41, <https://doi.org/10.1017/S0016756809990586>, 2010.
- Le Heron, D. P., Craig, J., Sutcliffe, O. E., and Whittington, R.: Late Ordovician glaciogenic reservoir heterogeneity: An example from the Murzuq Basin, Libya, *Mar. Petrol. Geol.*, 23, 655–677, <https://doi.org/10.1016/j.marpetgeo.2006.05.006>, 2006.
- Le Heron, D. P., Craig, J., and Etienne, J. L.: Ancient glaciations and hydrocarbon accumulations in North Africa and the Middle East, *Earth-Sci. Rev.*, 93, 47–76, <https://doi.org/10.1016/j.earscirev.2009.02.001>, 2009.
- Leeder, M. R.: Denudation, vertical crustal movements and sedimentary basin infill, *Geol. Rundsch.*, 80, 441–458, <https://doi.org/10.1007/BF01829376>, 1991.
- Légrand, P.: Le Dévonien du Sahara Algérien, *Can. Soc. Pet. Geol.*, 1, 245–284, 1967a.
- Légrand, P.: Nouvelles connaissances acquises sur la limite des systèmes Silurien et Dévonien au Sahara algérien, *Bull. Bur. Rech. Géologiques Minières*, 33, 119–37, 1967b.
- Légrand, P.: The lower Silurian graptolites of Oued In Djerane: a study of populations at the Ordovician–Silurian boundary, *Geol. Soc. Lond. Spec. Publ.*, 20, 145–153, <https://doi.org/10.1144/GSL.SP.1986.020.01.15>, 1986.

- Legrand, P.: Late Ordovician-early Silurian paleogeography of the Algerian Sahara, *Bull. Société Géologique Fr.*, 174, 19–32, 2003a.
- Legrand, P.: Silurian stratigraphy and paleogeography of the northern African margin of Gondwana, in: *Silurian Lands and Seas: Paleogeography Outside of Laurentia*, edited by: Landing, E. and Johnson, M. E., 59–104, New York, 2003b.
- Legrand-Blain, M.: *Dynamique des Brachiopodes carbonifères sur la plate-forme carbonatée du Sahara algérien: paléoenvironnements, paléobiogéographie, évolution*, Doctoral dissertation, Université de Bordeaux I, France, 1985.
- Lessa, G. and Masselink, G.: Morphodynamic evolution of a macrotidal barrier estuary, *Mar. Geol.*, 129, 25–46, 1995.
- Leuven, J. R. F. W., Kleinhans, M. G., Weisscher, S. A. H., and van der Vegt, M.: Tidal sand bar dimensions and shapes in estuaries, *Earth-Sci. Rev.*, 161, 204–223, <https://doi.org/10.1016/j.earscirev.2016.08.004>, 2016.
- Lewis, M. M., Jackson, C. A.-L., Gawthorpe, R. L., and Whipp, P. S.: Early synrift reservoir development on the flanks of extensional forced folds: A seismic-scale outcrop analog from the Hadahid fault system, Suez rift, Egypt, *AAPG Bull.*, 99, 985–1012, <https://doi.org/10.1306/12011414036>, 2015.
- Liégeois, J. P., Latouche, L., Boughrara, M., Navez, J., and Guiraud, M.: The LATEA metacraton (Central Hoggar, Tuareg shield, Algeria): behaviour of an old passive margin during the Pan-African orogeny, *J. Afr. Earth Sci.*, 37, 161–190, <https://doi.org/10.1016/j.jafrearsci.2003.05.004>, 2003.
- Liégeois, J.-P., Black, R., Navez, J., and Latouche, L.: Early and late Pan-African orogenies in the Air assembly of terranes (Tuareg Shield, Niger), *Precambrian Res.*, 67, 59–88, 1994.
- Liégeois, J.-P., Benhallou, A., Azzouni-Sekkal, A., Yahiaoui, R., and Bonin, B.: The Hoggar swell and volcanism: Reactivation of the Precambrian Tuareg shield during Alpine convergence and West African Cenozoic volcanism, *Geol. Soc. Am. Spec. Pap.*, 388, 379–400, <https://doi.org/10.1130/0-8137-2388-4.379>, 2005.
- Liégeois, J.-P., Abdelsalam, M. G., Ennih, N., and Ouabadi, A.: Metacraton: Nature, genesis and behavior, *Gondwana Res.*, 23, 220–237, <https://doi.org/10.1016/j.gr.2012.02.016>, 2013.
- Lindsay, J. F. and Leven, J. H.: Evolution of a Neoproterozoic to Palaeozoic intracratonic setting, Officer Basin, South Australia, *Basin Res.*, 8, 403–424, <https://doi.org/10.1046/j.1365-2117.1996.00223.x>, 1996.
- Logan, P. and Duddy, I.: An investigation of the thermal history of the Ahnet and Reggane Basins, Central Algeria, and the consequences for hydrocarbon generation and accumulation, *Geol. Soc. Lond. Spec. Publ.*, 132, 131–155, 1998.
- Loi, A., Ghienne, J.-F., Dabard, M. P., Paris, F., Botquelen, A., Christ, N., Elaouad-Debbaj, Z., Gorini, A., Vidal, M., Videt, B., and Destombes, J.: The Late Ordovician glacio-eustatic record from a high-latitude storm-dominated shelf succession: The Bou Ingarf section (Anti-Atlas, Southern Morocco), *Palaeogeogr. Palaeoclimatol.*, 296, 332–358, <https://doi.org/10.1016/j.palaeo.2010.01.018>, 2010.
- Lubeseder, S.: Silurian and Devonian sequence stratigraphy of North Africa; Regional correlation and sedimentology (Morocco, Algeria, Libya), Doctoral dissertation, University of Manchester, UK, 2005.
- Lubeseder, S., Redfern, J., Petitpierre, L., and Fröhlich, S.: Stratigraphic trapping potential in the Carboniferous of North Africa: developing new play concepts based on integrated outcrop sedimentology and regional sequence stratigraphy (Morocco, Algeria, Libya), in: *Geological Society, London, Petroleum Geology Conference series*, 7, 725–734, Geological Society of London, 2010.
- Lüning, S.: North African Phanerozoic, in: *Phanerozoic in the Northern African basins*, *Encyclopedia of Geology*, 152–172, Elsevier, 2005.
- Lüning, S., Craig, J., Loydell, D. K., Štorch, P., and Fitches, B.: Lower Silurian “hot shales” in North Africa and Arabia: regional distribution and depositional model, *Earth-Sci. Rev.*, 49, 121–200, [https://doi.org/10.1016/S0012-8252\(99\)00060-4](https://doi.org/10.1016/S0012-8252(99)00060-4), 2000.
- Lüning, S., Adamson, K., and Craig, J.: Frasnian organic-rich shales in North Africa: regional distribution and depositional model, *Geol. Soc. Lond. Spec. Publ.*, 207, 165–184, <https://doi.org/10.1144/GSL.SP.2003.207.9>, 2003.
- Lüning, S., Wendt, J., Belka, Z., and Kaufmann, B.: Temporal-spatial reconstruction of the early Frasnian (Late Devonian) anoxia in NW Africa: new field data from the Ahnet Basin (Algeria), *Sediment. Geol.*, 163, 237–264, [https://doi.org/10.1016/S0037-0738\(03\)00210-0](https://doi.org/10.1016/S0037-0738(03)00210-0), 2004.
- Madritsch, H., Schmid, S. M., and Fabbri, O.: Interactions between thin-and thick-skinned tectonics at the northwestern front of the Jura fold-and-thrust belt (eastern France), *Tectonics*, 27, 1–31, <https://doi.org/10.1029/2008TC002282>, 2008.
- Magloire, L.: Étude stratigraphique, par la Palynologie, des dépôts argilo-gréseux du Silurien et du Dévonien inférieur dans la Région du Grand Erg Occidental (Sahara Algérien), *Can. Soc. Pet. Geol.*, 2, 473–491, 1967.
- Makhous, M. and Galushkin, Y. I.: Burial history and thermal evolution of the northern and eastern Saharan basins, *AAPG Bull.*, 87, 1623–1651, <https://doi.org/10.1306/04300301122>, 2003a.
- Makhous, M. and Galushkin, Y. I.: Burial history and thermal evolution of the southern and western Saharan basins: Synthesis and comparison with the eastern and northern Saharan basins, *AAPG Bull.*, 87, 1799–1822, 2003b.
- Marchal, D., Guiraud, M., Rives, T., and van den Driessche, J.: Space and time propagation processes of normal faults, *Geol. Soc. Lond. Spec. Publ.*, 147, 51–70, <https://doi.org/10.1144/GSL.SP.1998.147.01.04>, 1998.
- Marchal, D., Guiraud, M., and Rives, T.: Geometric and morphologic evolution of normal fault planes and traces from 2D to 4D data, *J. Struct. Geol.*, 25, 135–158, [https://doi.org/10.1016/S0191-8141\(02\)00011-1](https://doi.org/10.1016/S0191-8141(02)00011-1), 2003.
- Massa, D.: Paléozoïque de Libye occidentale?: stratigraphie et paléogéographie, Doctoral dissertation, Université de Nice, France, 1988.
- Mélou, M., Oulebsir, L., and Paris, F.: Brachiopodes et chitinozoaires ordoviciens dans le NE du Sahara algérien: Implications stratigraphiques et paléogéographiques, *Geobios*, 32, 822–839, [https://doi.org/10.1016/S0016-6995\(99\)80865-1](https://doi.org/10.1016/S0016-6995(99)80865-1), 1999.
- Milani, E. J. and Zalan, P. V.: An outline of the geology and petroleum systems of the Paleozoic interior basins of South America, *Episodes*, 22, 199–205, 1999.
- Milton, N. J., Bertram, G. T., and Vann, I. R.: Early Palaeogene tectonics and sedimentation in the Central North Sea, *Geol. Soc. Lond. Spec. Publ.*, 55, 339–351, 1990.

- Moreau, C., Demaiffe, D., Bellion, Y., and Boullier, A.-M.: A tectonic model for the location of Palaeozoic ring complexes in Air (Niger, West Africa), *Tectonophysics*, 234, 129–146, 1994.
- Mory, A. J., Zhan, Y., Haines, P. W., Hocking, R. M., Thomas, C. M., and Copp, I. A.: A paleozoic perspective of Western Australia, Geological Survey of Western Australia, 2017.
- Najem, A., El-Arnauti, A., and Bosnina, S.: Delineation of Paleozoic Tecto-stratigraphic Complexities in the Northern Part of Murzuq Basin-Southwest Libya, in SPE North Africa Technical Conference and Exhibition, Society of Petroleum Engineers, 2015.
- Nikishin, A. M., Ziegler, P. A., Stephenson, R. A., Cloetingh, S., Furne, A. V., Fokin, P. A., Ershov, A. V., Bolotov, S. N., Korotaev, M. V., and Alekseev, A. S.: Late Precambrian to Triassic history of the East European Craton: dynamics of sedimentary basin evolution, *Tectonophysics*, 268, 23–63, 1996.
- Ogg, J. G., Ogg, G., and Gradstein, F. M.: Introduction, in *A Concise Geologic Time Scale*: 2016, p. 3, Elsevier, 2016.
- Oudra, M., Beraaouz, H., Ikenne, M., Gasquet, D., and Soulaïmani, A.: La Tectonique Panafricaine du Secteur d'Igherm: Implication des dômes extensifs tardi à post-orogéniques (Anti-Atlas occidental, Maroc), *Estud. Geológicas*, 61, 177–189, 2005.
- Oulebsir, L. and Paris, F.: Chitinozoaires ordoviciens du Sahara algérien: biostratigraphie et affinités paléogéographiques, *Rev. Palaeobot. Palyno.*, 86, 49–68, [https://doi.org/10.1016/0034-6667\(94\)00098-5](https://doi.org/10.1016/0034-6667(94)00098-5), 1995.
- Owen, G.: Senni Beds of the Devonian Old Red Sandstone, Dyfed, Wales: anatomy of a semi-arid floodplain, *Sediment. Geol.*, 95, 221–235, 1995.
- Paris, F.: The Ordovician chitinozoan biozones of the Northern Gondwana domain, *Rev. Palaeobot. Palyno.*, 66, 181–209, [https://doi.org/10.1016/0034-6667\(90\)90038-K](https://doi.org/10.1016/0034-6667(90)90038-K), 1990.
- Paris, F., Bourahrouh, A., and Hérisse, A. L.: The effects of the final stages of the Late Ordovician glaciation on marine palynomorphs (chitinozoans, acritarchs, leiospheres) in well NI-2 (NE Algerian Sahara), *Rev. Palaeobot. Palyno.*, 113, 87–104, [https://doi.org/10.1016/S0034-6667\(00\)00054-3](https://doi.org/10.1016/S0034-6667(00)00054-3), 2000.
- Peace, A., McCaffrey, K., Imber, J., van Hunen, J., Hobbs, R., and Wilson, R.: The role of pre-existing structures during rifting, continental breakup and transform system development, offshore West Greenland, *Basin Res.*, 30, 373–394, 2018.
- Pemberton, S. G. and Frey, R. W.: Trace fossil nomenclature and the Planolites-Palaeophycus dilemma, *J. Paleontol.*, 56, 843–881, 1982.
- Peucat, J. J., Drareni, A., Latouche, L., Deloule, E., and Vidal, P.: U–Pb zircon (TIMS and SIMS) and Sm–Nd whole-rock geochronology of the Gour Oumelalen granulitic basement, Hoggar massif, Tuareg shield, Algeria, *J. Afr. Earth Sci.*, 37, 229–239, <https://doi.org/10.1016/j.jafrearsci.2003.03.001>, 2003.
- Peucat, J.-J., Capdevila, R., Drareni, A., Mahdjoub, Y., and Kahoui, M.: The Eglab massif in the West African Craton (Algeria), an original segment of the Eburnean orogenic belt: petrology, geochemistry and geochronology, *Precambrian Res.*, 136, 309–352, <https://doi.org/10.1016/j.precamres.2004.12.002>, 2005.
- Phillips, T. B., Jackson, C. A.-L., Bell, R. E., and Duffy, O. B.: Oblique reactivation of lithosphere-scale lineaments controls rift physiography – the upper-crustal expression of the Sorgenfrei-Tornquist Zone, offshore southern Norway, *Solid Earth*, 9, 403–429, <https://doi.org/10.5194/se-9-403-2018>, 2018.
- Pinet, N., Lavoie, D., Dietrich, J., Hu, K., and Keating, P.: Architecture and subsidence history of the intracratonic Hudson Bay Basin, northern Canada, *Earth-Sci. Rev.*, 125, 1–23, <https://doi.org/10.1016/j.earscirev.2013.05.010>, 2013.
- Potter, D.: Relationships of Cambro-Ordovician Stratigraphy to Paleotopography on the Precambrian Basement, Williston Basin, *Sask. Geol. Soc.*, 63–73, 2006.
- Reading, H. G. and Collinson, J. D.: Clastic coasts, in *Sedimentary environments: processes, facies, and stratigraphy*, 154–231, John Wiley & Sons, Oxford; Cambridge, Mass., 2009.
- Rider, M. H.: Facies, Sequences and Depositional Environments from Logs, in *The geological interpretation of well logs*, 226–238, Whittles Publishing, Caithness, Scotland, 1996.
- Rougier, S., Missenard, Y., Gautheron, C., Barbarand, J., Zeyen, H., Pinna, R., Liégeois, J.-P., Bonin, B., Ouabadi, A., Derder, M. E.-M., and Lamotte, D. F. de: Eocene exhumation of the Tuareg Shield (Sahara Desert, Africa), *Geology*, 41, 615–618, <https://doi.org/10.1130/G33731.1>, 2013.
- Sabaou, N., Ait-Salem, H., and Zazoun, R. S.: Chemostratigraphy, tectonic setting and provenance of the Cambro-Ordovician clastic deposits of the subsurface Algerian Sahara, *J. Afr. Earth Sci.*, 55, 158–174, <https://doi.org/10.1016/j.jafrearsci.2009.04.006>, 2009.
- Schlische, R. W.: Geometry and origin of fault-related folds in extensional settings, *AAPG Bull.*, 79, 1661–1678, 1995.
- Sclater, J. G. and Christie, P. A. F.: Continental stretching: An explanation of the Post-Mid-Cretaceous subsidence of the central North Sea Basin, *J. Geophys. Res.-Sol. Ea.*, 85, 3711–3739, <https://doi.org/10.1029/JB085iB07p03711>, 1980.
- Scotese, C. R., Boucot, A. J., and McKerrow, W. S.: Gondwanan palaeogeography and paleoclimatology, *J. Afr. Earth Sci.*, 28, 99–114, [https://doi.org/10.1016/S0899-5362\(98\)00084-0](https://doi.org/10.1016/S0899-5362(98)00084-0), 1999.
- Serra, O. and Serra, L.: Well logging, facies, sequence and environment, in *Well logging and geology*, 197–238, Technip Editions, France, 2003.
- Sharata, S., Röth, J., and Reicherter, K.: Basin evolution in the North African Platform, *Geotecton. Res.*, 97, 80–81, <https://doi.org/10.1127/1864-5658/2015-31>, 2015.
- Shaw, J. H., Connors, C. D., and Suppe, J.: Recognizing growth strata, in *Seismic interpretation of contractional fault-related folds: an AAPG seismic atlas*, 53, 11–14, American Association of Petroleum Geologists, Tulsa, Okla, USA, 2005.
- Sloss, L. L.: Sequences in the cratonic interior of North America, *Geol. Soc. Am. Bull.*, 74, 93–114, 1963.
- Smart, J.: Seismic expressions of depositional processes in the upper Ordovician succession of the Murzuq Basin, SW Libya, in: *Geological Exploration in Murzuq Basin*, edited by: Sola, M. A. and Worsley, D., 397–415, Elsevier Science B.V., Amsterdam., 2000.
- Soares, P. C., Landim, P. M. B., and Fulfaro, V. J.: Tectonic cycles and sedimentary sequences in the Brazilian intracratonic basins, *GSA Bull.*, 89, 181–191, [https://doi.org/10.1130/0016-7606\(1978\)89<181:TCASSI>2.0.CO;2](https://doi.org/10.1130/0016-7606(1978)89<181:TCASSI>2.0.CO;2), 1978.
- Stearns, D. W.: Faulting and forced folding in the Rocky Mountains foreland, Laramide Fold. Assoc. Basement Block Faulting West, *US Geol. Soc. Am. Mem.*, 151, 1–37, 1978.
- Stow, D. A. V. and Piper, D. J. W.: Deep-water fine-grained sediments: facies models, *Geol. Soc. Lond. Spec. Publ.*, 15, 611–646, <https://doi.org/10.1144/GSL.SP.1984.015.01.38>, 1984.

- Stow, D. A. V., Huc, A.-Y., and Bertrand, P.: Depositional processes of black shales in deep water, *Mar. Petrol. Geol.*, 18, 491–498, [https://doi.org/10.1016/S0264-8172\(01\)00012-5](https://doi.org/10.1016/S0264-8172(01)00012-5), 2001.
- Suter, J. R.: Facies models revisited: clastic shelves, *Spec. Publ.-SEPM*, 84, 339–398, 2006.
- Tournier, F.: Mécanismes et contrôle des phénomènes diagénétiques en milieu acide dans les grès de l'Ordovicien glaciaire du bassin de Sbaa, Algérie, Doctoral dissertation, Université de Paris 11, France, 2010.
- Trompette, R.: Gondwana evolution; its assembly at around 600 Ma, *Comptes Rendus Académie Sci.-Ser. IIA-Earth Planet. Sci.*, 330, 305–315, 2000.
- Turner, G. M., Rasson, J. L., and Reeves, C. V.: Observation and Measurement Techniques, in *Treatise on Geophysics*, 5, edited by: Schubert, G., 33–75, Blackwell Pub, Malden, MA., 2007.
- Ustaszewski, K., Schumacher, M., Schmid, S., and Nieuwland, D.: Fault reactivation in brittle–viscous wrench systems—dynamically scaled analogue models and application to the Rhine–Bresse transfer zone, *Quaternary Sci. Rev.*, 24, 363–380, <https://doi.org/10.1016/j.quascirev.2004.03.015>, 2005.
- Van Hinte, J. E.: Geohistory analysis—application of micropaleontology in exploration geology, *AAPG Bull.*, 62, 201–222, 1978.
- Vauchez, A., Tommasi, A., and Barruol, G.: Rheological heterogeneity, mechanical anisotropy and deformation of the continental lithosphere, *Tectonophysics*, 296, 61–86, [https://doi.org/10.1016/S0040-1951\(98\)00137-1](https://doi.org/10.1016/S0040-1951(98)00137-1), 1998.
- Vecoli, M.: Palaeoenvironmental interpretation of microphytoplankton diversity trends in the Cambrian–Ordovician of the northern Sahara Platform, *Palaeogeogr. Palaeoclimatol.*, 160, 329–346, [https://doi.org/10.1016/S0031-0182\(00\)00080-8](https://doi.org/10.1016/S0031-0182(00)00080-8), 2000.
- Vecoli, M. and Playford, G.: Stratigraphically significant acritarchs in uppermost Cambrian to basal Ordovician strata of Northwestern Algeria, *Grana*, 36, 17–28, <https://doi.org/10.1080/00173139709362585>, 1997.
- Vecoli, M., Albani, R., Ghomari, A., Massa, D., and Tongiorgi, M.: Précisions sur la limite Cambrien-Ordovicien au Sahara Algérien (Secteur de Hassi-Rmel), *Comptes Rendus Académie Sci. Sér. 2 Sci. Terre Planètes*, 320, 515–522, 1995.
- Vecoli, M., Tongiorgi, M., Abdesselam-Roughi, F. F., Benzarti, R., and Massa, D.: Palynostratigraphy of upper Cambrian–upper Ordovician intracratonic clastic sequences, North Africa, *Boll.-Soc. Paleontol. Ital.*, 38, 331–342, 1999.
- Vecoli, M., Videt, B., and Paris, F.: First biostratigraphic (palynological) dating of Middle and Late Cambrian strata in the subsurface of northwestern Algeria, North Africa: Implications for regional stratigraphy, *Rev. Palaeobot. Palynol.*, 149, 57–62, <https://doi.org/10.1016/j.revpalbo.2007.10.004>, 2008.
- Videt, B., Paris, F., Rubino, J.-L., Boumendjel, K., Dabard, M.-P., Loi, A., Ghienne, J.-F., Marante, A., and Gorini, A.: Biostratigraphical calibration of third order Ordovician sequences on the northern Gondwana platform, *Palaeogeogr. Palaeoclimatol.*, 296, 359–375, <https://doi.org/10.1016/j.palaeo.2010.03.050>, 2010.
- Wagoner, J. C. V., Mitchum, R. M., Campion, K. M., and Rahmanian, V. D.: Siliciclastic Sequence Stratigraphy in Well Logs, Cores, and Outcrops: Concepts for High-Resolution Correlation of Time and Facies, *AAPG Methods Explor. Ser. No 7*, 174, III–55, 1990.
- Watts, A. B.: *Isostasy and Flexure of the Lithosphere*, Cambridge University Press, Oxford University, 2001.
- Wendt, J.: Disintegration of the continental margin of northwestern Gondwana: Late Devonian of the eastern Anti-Atlas (Morocco), *Geology*, 13, 815–818, 1985.
- Wendt, J.: Facies Pattern and Paleogeography of the Middle and Late Devonian in the Eastern Anti-Atlas (Morocco), *Can. Soc. Pet. Geol.*, 1, 467–480, 1988.
- Wendt, J.: Shell directions as a tool in palaeocurrent analysis, *Sediment. Geol.*, 95, 161–186, [https://doi.org/10.1016/0037-0738\(94\)00104-3](https://doi.org/10.1016/0037-0738(94)00104-3), 1995.
- Wendt, J. and Kaufmann, B.: Mud buildups on a Middle Devonian carbonate ramp (Algerian Sahara), *Geol. Soc. Lond. Spec. Publ.*, 149, 397–415, <https://doi.org/10.1144/GSL.SP.1999.149.01.18>, 1998.
- Wendt, J., Belka, Z., and Moussine-Pouchkine, A.: New architectures of deep-water carbonate buildups: Evolution of mud mounds into mud ridges (Middle Devonian, Algerian Sahara), *Geology*, 21, 723–726, 1993.
- Wendt, J., Belka, Z., Kaufmann, B., Kostrewa, R., and Hayer, J.: The world's most spectacular carbonate mud mounds (Middle Devonian, Algerian Sahara), *J. Sediment. Res.*, 67, 424–436, <https://doi.org/10.1306/D426858B-2B26-11D7-8648000102C1865D>, 1997.
- Wendt, J., Kaufmann, B., Belka, Z., Klug, C., and Lubeseder, S.: Sedimentary evolution of a Palaeozoic basin and ridge system: the Middle and Upper Devonian of the Ahnet and Mouydir (Algerian Sahara), *Geol. Mag.*, 143, 269–299, <https://doi.org/10.1017/S0016756806001737>, 2006.
- Wendt, J., Kaufmann, B., Belka, Z., and Korn, D.: Carboniferous stratigraphy and depositional environments in the Ahnet Mouydir area (Algerian Sahara), *Facies*, 55, 443–472, <https://doi.org/10.1007/s10347-008-0176-y>, 2009a.
- Wendt, J., Kaufmann, B., and Belka, Z.: Devonian stratigraphy and depositional environments in the southern Illizi Basin (Algerian Sahara), *J. Afr. Earth Sci.*, 54, 85–96, <https://doi.org/10.1016/j.jafrearsci.2009.03.006>, 2009b.
- Withjack, M. O. and Callaway, S.: Active normal faulting beneath a salt layer: an experimental study of deformation patterns in the cover sequence, *AAPG Bull.*, 84, 627–651, 2000.
- Withjack, M. O., Olson, J., and Peterson, E.: Experimental models of extensional forced folds, *AAPG Bull.*, 74, 1038–1054, 1990.
- Withjack, M. O., Schlische, R. W., and Olsen, P. E.: Rift-basin structure and its influence on sedimentary systems, *Soc. Sediment. Geol. Spec. Publ.*, 73, 57–81, 2002.
- Xie, X. and Heller, P.: Plate tectonics and basin subsidence history, *Geol. Soc. Am. Bull.*, 121, 55–64, <https://doi.org/10.1130/B26398.1>, 2009.
- Yahi, N.: Petroleum generation and migration in the Berkine (Ghadames) Basin, Eastern Algeria: an organic geochemical and basin modelling study, Doctoral dissertation, Forschungszentrum, Zentralbibliothek, Jülich, 1999.
- Zalan, P. V., Wolff, S., Astolfi, M. A. M., Vieira, I. S., Concelcao, J. C. J., Appi, V. T., Neto, E. V. S., Cerqueira, J. R., and Marques, A.: The Parana Basin, Brazil: Chapter 33: Part II. Selected Analog Interior Cratonic Basins: Analog Basins, 134, 681–708, 1990.
- Zazoun, R. S.: Hercynian deformation in the western Ahnet Basin and Bled El-Mass area, Algerian Sahara: a continuous strain, *J. Afr. Earth Sci.*, 32, 869–887, 2001.

Zazoun, R. S.: The Fadnoun area, Tassili-n-Azdjer, Algeria: Fracture network geometry analysis, *J. Afr. Earth Sci.*, 50, 273–285, <https://doi.org/10.1016/j.jafrearsci.2007.10.001>, 2008.

Zazoun, R. S. and Mahdjoub, Y.: Strain analysis of Late Ordovician tectonic events in the In-Tahouite and Tamadjert Formations (Tassili-n-Ajers area, Algeria), *J. Afr. Earth Sci.*, 60, 63–78, <https://doi.org/10.1016/j.jafrearsci.2011.02.003>, 2011.